DOA estimation for noncircular signals : performance bounds and algorithms

Jean-Pierre Delmas, Habti Abeida

DOA estimation for noncircular signals: performance bounds and algorithms

Jean-Pierre Delmas, Habti Abeida
Département CITI, UMR-CNRS 5157,
Institut National des Télécommunications, Evry, France

9.1 Introduction

There is considerable literature about second-order statistics-based algorithms for estimating directions of arrival (DOA) of narrowband sources impinging on an array of sensors. These algorithms, however, have been examined under the complex circular Gaussian assumption only. The interest in these algorithms stems from a large number of applications including mobile communications systems [1]. In this application, after frequency down-shifting the sensor signals to baseband, the in-phase and quadrature components are paired to obtain complex signals. Complex noncircular signals [2], such as, binary phase shift keying (BPSK) and offset quadrature phase shift keying (OQPSK) modulated signals, are often used. Naturally, the second-order algorithms devoted to complex circular signals relying on the positive definite Hermitian covariance matrix $\mathrm{E}(\mathbf{y}_t\mathbf{y}_t^H)$ can be used in this context. But because the second-order statistical characteristics are also contained in the complex symmetric unconjugated spatial covariance matrix $\mathrm{E}(\mathbf{y}_t\mathbf{y}_t^T)$ for noncircular signals, a potentially performance improvement ought to be obtained if these two covariance matrices are used. However, only a few contributions (among them, [3, 4, 5]) have been devoted to noncircular signals in DOA estimation in the last years.

The aim of this chapter is to present an overview of algorithms and performance bounds of DOA estimates of noncircular signals. This chapter is organized as follows. The array signal model with some notations and the statement of the problem are given in Section 2. The potential benefit due to the noncircularity property is underscored by the help of subspace-based algorithms built from the unconjugated spatial covariance matrix only. Three attractive multiple signal classification (MUSIC)-like algorithms and an optimally weighted MUSIC algorithm built from the two covariance matrices are then presented with their asymptotic performances in Section 3. To assess the performance and efficiency of these algorithms, asymptotically (in the number of measurements) minimum variance (AMV) algorithms in the class of consistent algorithms based on the two covariance matrices or on their associated orthogonal projectors and AMV bounds are described in Section 4. Because the Gaussian stochastic Cramer-Rao bound (CRB) matrix is, under rather general conditions, the largest of all CRB matrices among the class of arbitrary distributions with given mean and covariance (see e.g., [6, p. 293]), the noncircular Gaussian stochastic CRB is derived in Section 5 as a tight upper bound of the stochastic CRB under discrete distributions. The case of BPSK sources is specifically treated in Section 6. Finally, this chapter ends by illustrative exemples and conclusion.

9.2 Array signal model

Let an array of M sensors receive the signals emitted by K narrowband sources. The observation vectors are modelled as

$$\mathbf{y}_t = \mathbf{A}\mathbf{x}_t + \mathbf{n}_t, \qquad t = 1, \ldots, T,$$

where $(\mathbf{y}_t)_{t=1,\ldots,T}$ are independent and identically distributed. $\mathbf{A}(\boldsymbol{\theta}) = [\mathbf{a}_1, \ldots, \mathbf{a}_K]$ is the steering matrix where each vector $\mathbf{a}_k = \mathbf{a}(\theta_k)$ is parameterized by the real scalar parameter θ_k to avoid unnecessary notational complexity, but the results presented here apply to a general parameterization. $\mathbf{x}_t = (x_{t,1}, \ldots, x_{t,K})^T$ and $\mathbf{n}_t$ model the source signals and additive measurement noise respectively. $\mathbf{x}_t$ and $\mathbf{n}_t$ are multivariate independent and zero-mean. $\mathbf{n}_t$ is assumed Gaussian complex circular, spatially uniformly uncorrelated with $\mathrm{E}(\mathbf{n}_t\mathbf{n}_t^H) = \sigma_n^2\mathbf{I}_M$ or spatially correlated with unknown covariance matrix $\mathrm{E}(\mathbf{n}_t\mathbf{n}_t^H) = \mathbf{Q}_n(\boldsymbol{\sigma})$ parameterized by the vector of real unknown coefficients $\boldsymbol{\sigma} \stackrel{\text{def}}{=} (\sigma_1 \ldots, \sigma_N)^T$. This general noise model was introduced in [7] and used in [8] and [9]. $\mathbf{x}_t$ is complex noncircular, not necessarily Gaussian, and possibly spatially correlated or even coherent with spatial covariance matrices $\mathbf{R}_x \stackrel{\text{def}}{=} \mathrm{E}(\mathbf{x}_t\mathbf{x}_t^H)$ and $\mathbf{R}'_x \stackrel{\text{def}}{=} \mathrm{E}(\mathbf{x}_t\mathbf{x}_t^T)$. Consequently, this leads to two covariance matrices of $\mathbf{y}_t$ that contain information about $\boldsymbol{\theta} \stackrel{\text{def}}{=} (\theta_1, \ldots, \theta_K)^T$:

$$\mathbf{R}_y = \mathbf{A}\mathbf{R}_x\mathbf{A}^H + \mathbf{Q}_n \qquad \text{and} \qquad \mathbf{R}'_y = \mathbf{A}\mathbf{R}'_x\mathbf{A}^T \neq \mathbf{O}. \tag{9.1}$$

If no a priori information is available concerning the spatial covariance of the sources, $\mathbf{R}_x$ and $\mathbf{R}'_x$ are generically parameterized by the real parameters $\boldsymbol{\rho} = ((\Re([\mathbf{R}_x]_{i,j}), \Im([\mathbf{R}_x]_{i,j}), \Re([\mathbf{R}'_x]_{i,j}), \Im([\mathbf{R}'_x]_{i,j}))_{1\leq j<i\leq K}, ([\mathbf{R}_x]_{i,i}, \Re([\mathbf{R}'_x]_{i,i}), \Im([\mathbf{R}'_x]_{i,i}))_{i=1,\ldots,K})^T$. Thus the couple $(\mathbf{R}_y, \mathbf{R}'_y)$ is parameterized by the real parameter $\boldsymbol{\alpha} \stackrel{\text{def}}{=} (\boldsymbol{\theta}^T, \boldsymbol{\rho}^T, \boldsymbol{\sigma}^T)^T \in \mathbb{R}^L$. This parameter is assumed identifiable from $\big(\mathbf{R}_y(\boldsymbol{\alpha}), \mathbf{R}'_y(\boldsymbol{\alpha})\big)$, in the following sense:

$$\mathbf{R}_y(\boldsymbol{\alpha}) = \mathbf{R}_y(\boldsymbol{\alpha}') \qquad \text{and} \qquad \mathbf{R}'_y(\boldsymbol{\alpha}) = \mathbf{R}'_y(\boldsymbol{\alpha}') \qquad \Rightarrow \qquad \boldsymbol{\alpha} = \boldsymbol{\alpha}'.$$

These covariance matrices are traditionally estimated by $\mathbf{R}_{y,T} = \frac{1}{T}\sum_{t=1}^T \mathbf{y}_t\mathbf{y}_t^H$ and $\mathbf{R}'_{y,T} = \frac{1}{T}\sum_{t=1}^T \mathbf{y}_t\mathbf{y}_t^T$, respectively.

For a performance analysis, some extra hypotheses are needed. We suppose that the signal waveforms stem from $\bar{K}$ independent signals $\bar{x}_{t,k}$, with $\bar{K} \leq K$, with strict inequality implying linear dependence among the signal waveforms emanating from, e.g., specular multipath or smart jamming in communication applications. We suppose that the signal waveforms have finite fourth-order moments. The noncircularity rate ρ_k of the kth source is defined by $\mathrm{E}(x_{t,k}^2) = \rho_k e^{i\phi_k}\sigma_{s_k}^2$ where ϕ_k is its circularity phase that satisfies $0 \leq \rho_k \leq 1$ and $\sigma_{s_k}^2 \stackrel{\text{def}}{=} \mathrm{E}|s_{t,k}^2|$.

The problem of interest in this work concerns estimating $\boldsymbol{\theta}$ from the two sample covariance matrices $\mathbf{R}_{y,T}$ and $\mathbf{R}'_{y,T}$. The number K of sources is assumed to be known.

9.3 MUSIC-like algorithms

We suppose in this section that $\mathbf{Q}_n = \sigma_n^2\mathbf{I}_M$, $\mathbf{A}$ is full column rank and $\mathbf{R}_x$ and $\mathbf{R}'_x$ are nonsingular. To prove the potential benefit due to the noncircularity of the sources, we first propose MUSIC-like algorithms built from the unconjugated spatial covariance matrix only.

9.3.1 MUSIC-like algorithms built from $\mathbf{R}'_{y,T}$ only

Because $\mathbf{R}'_y$ and $\mathbf{R}_y$ have a common noise subspace (see (9.1)) with associated orthogonal projection matrices $\boldsymbol{\Pi}' = \boldsymbol{\Pi}$, the first idea for estimating $\boldsymbol{\theta}$ from $\mathbf{R}'_{y,T}$ alone is to apply the following steps: Estimate the projection matrix $\boldsymbol{\Pi}'_T$ associated with the noise subspace of $\mathbf{R}'_{y,T}$ by the singular value decomposition of the symmetric complex-valued matrix $\mathbf{R}'_{y,T}$ and then, use the standard MUSIC algorithm based on $\boldsymbol{\Pi}'_T$ where the DOA $(\theta_{k,T})_{k=1,\ldots,K}$ are estimated as the locations of the K smallest minima of the function:

$$\theta_{k,T}^{\mathrm{Alg}_0} = \arg\min_{\theta} \ \mathbf{a}^H(\theta)\boldsymbol{\Pi}'_T\mathbf{a}(\theta). \tag{9.2}$$

Compared to the standard MUSIC algorithm based on $\boldsymbol{\Pi}_T$ associated with the noise subspace of $\mathbf{R}_{y,T}$, we prove in [10] the following

Theorem 1 *The sequences $\sqrt{T}(\boldsymbol{\theta}_T - \boldsymbol{\theta})$, where $\boldsymbol{\theta}_T$ is the DOA estimate given by these two standard MUSIC algorithms, converge in distribution to the zero-mean Gaussian distribution of covariance matrix of the similar structure*

$$(\mathbf{C}_{\boldsymbol{\theta}})_{k,l} = \frac{2}{\alpha_k \alpha_l} \Re\left(\left(\mathbf{a}_l^H \mathbf{U} \mathbf{a}_k \right) \left(\mathbf{a}_k^{'H} \boldsymbol{\Pi} \mathbf{a}_l^{'} \right) \right) \tag{9.3}$$

with $\mathbf{a}_k^{'} \stackrel{\text{def}}{=} \frac{d\mathbf{a}_k}{d\theta_k}$ and $\alpha_k \stackrel{\text{def}}{=} 2\mathbf{a}_k^{'H} \boldsymbol{\Pi} \mathbf{a}_k^{'}$, where $\mathbf{U} \stackrel{\text{def}}{=} \sigma_n^2 \mathbf{S}^{\#} \mathbf{R}_y \mathbf{S}^{\#}$ with $\mathbf{S} \stackrel{\text{def}}{=} \mathbf{A}\mathbf{R}_x\mathbf{A}^H$ and $\mathbf{U} \stackrel{\text{def}}{=} \sigma_n^2 \mathbf{S}'^{\#} \mathbf{R}_y^T \mathbf{S}'^{*\#}$ with $\mathbf{S}' \stackrel{\text{def}}{=} \mathbf{A}\mathbf{R}_x'\mathbf{A}^T$ for the MUSIC algorithms built on $\mathbf{R}_{y,T}$ and $\mathbf{R}'_{y,T}$ respectively.

As a result, the asymptotic performance of the estimates given by these two standard MUSIC algorithms can be very similar. In particular, for only one source, it is proved in [10] that these asymptotic variances are respectively given by:

$$C_{\theta_1} = \frac{1}{\alpha_1 r_1} \left(1 + \frac{1}{\|\mathbf{a}_1\|^2 r_1} \right) \qquad \text{and} \qquad C_{\theta_1} = \frac{1}{\alpha_1 r_1 \rho_1^2} \left(1 + \frac{1}{\|\mathbf{a}_1\|^2 r_1} \right),$$

with $r_1 \stackrel{\text{def}}{=} \frac{\sigma_{s1}^2}{\sigma_n^2}$. We note that for $\rho_1 = 1$ (e.g., for an unfiltered BPSK modulated source), these two variances are equal. Naturally when ρ_1 approaches zero, C_{θ_1} is unbounded and the unconjugated spatial covariance matrix $\mathbf{R}'_y$ conveys no information about θ_1. This result raises the following query: how does one combine the statistics $\boldsymbol{\Pi}_T$ and $\boldsymbol{\Pi}'_T$ to improve the estimate of $\boldsymbol{\theta}$? A possible solution is proposed in the following subsection.

9.3.2 MUSIC-like algorithms built from both $\mathbf{R}_{y,T}$ and $\mathbf{R}'_{y,T}$

To devise simple subspace-based algorithms built from both $\mathbf{R}_{y,T}$ and $\mathbf{R}'_{y,T}$, we consider the extended covariance matrix $\mathbf{R}_{\tilde{y}} \stackrel{\text{def}}{=} \mathrm{E}(\tilde{\mathbf{y}}_t \tilde{\mathbf{y}}_t^H)$ where $\tilde{\mathbf{y}}_t \stackrel{\text{def}}{=} \left(\mathbf{y}_t^T, \mathbf{y}_t^{'H} \right)^T$ for which:

$$\mathbf{R}_{\tilde{y}} = \tilde{\mathbf{A}} \mathbf{R}_{\tilde{x}} \tilde{\mathbf{A}}^H + \sigma_n^2 \mathbf{I}_{2M} \tag{9.4}$$

with $\tilde{\mathbf{A}} \stackrel{\text{def}}{=} \begin{pmatrix} \mathbf{A} & \mathbf{O} \\ \mathbf{O} & \mathbf{A}^* \end{pmatrix}$ and $\mathbf{R}_{\tilde{x}} \stackrel{\text{def}}{=} \begin{pmatrix} \mathbf{R}_x & \mathbf{R}_x^{'} \\ \mathbf{R}_x^{'*} & \mathbf{R}_x^* \end{pmatrix}$. From the assumptions of Section 3, $K \leq \mathrm{rank}(\mathbf{R}_{\tilde{x}}) \leq 2K$ and, depending on this rank, many situations may be considered. We concentrate first on a particular case (case (1)) for which the sources are uncorrelated and with noncircularity rate ρ_k equal to 1 because very attractive algorithms have been devised for this case [3],[4]. This corresponds, for example, to unfiltered BPSK or OQPSK uncorrelated modulated signals. In this case, $\mathbf{R}_x = \boldsymbol{\Delta}_\sigma$ and $\mathbf{R}_x^{'} = \boldsymbol{\Delta}_\sigma \boldsymbol{\Delta}_\phi$ with $\boldsymbol{\Delta}_\sigma \stackrel{\text{def}}{=} \mathrm{Diag}(\sigma_{s_1}^2, \ldots, \sigma_{s_K}^2)$ and $\boldsymbol{\Delta}_\phi \stackrel{\text{def}}{=} \mathrm{Diag}(e^{i\phi_1}, \ldots, e^{i\phi_K})$. Consequently

$$\mathbf{R}_{\tilde{x}} = \begin{pmatrix} \boldsymbol{\Delta}_\sigma & \boldsymbol{\Delta}_\sigma \boldsymbol{\Delta}_\phi \\ \boldsymbol{\Delta}_\sigma \boldsymbol{\Delta}_\phi^* & \boldsymbol{\Delta}_\sigma \end{pmatrix} = \begin{pmatrix} \mathbf{I}_K \\ \boldsymbol{\Delta}_\phi^* \end{pmatrix} \boldsymbol{\Delta}_\sigma \begin{pmatrix} \mathbf{I}_K \\ \boldsymbol{\Delta}_\phi^* \end{pmatrix}^H$$

and $\mathrm{rank}(\mathbf{R}_{\tilde{x}}) = K$. Then subsequently, we consider the general case for which $\mathrm{rank}(\mathbf{R}_{\tilde{x}}) = 2K$ (case (2)). This case corresponds for example to filtered BPSK or OQPSK modulated signals. In these two cases, the orthogonal projector matrix onto the noise subspace is structured as $\tilde{\mathbf{A}}$ and $\mathbf{R}_{\tilde{x}}$. More precisely, the following lemma is proved in [10]

Lemma 1 *In cases (1) and (2), the orthogonal projector matrix $\tilde{\boldsymbol{\Pi}}$ onto the noise subspace is structured as*

$$\tilde{\boldsymbol{\Pi}} = \begin{pmatrix} \boldsymbol{\Pi}_1 & \boldsymbol{\Pi}_2 \\ \boldsymbol{\Pi}_2^* & \boldsymbol{\Pi}_1^* \end{pmatrix}$$

where $\mathbf{\Pi}_1$ *and* $\mathbf{\Pi}_2$ *are Hermitian and complex symmetric, respectively, and where* $\mathbf{\Pi}_1$ *is the orthogonal projector onto the column space of* $\mathbf{A}$ *and* $\mathbf{\Pi}_2 = \mathbf{O}$ *in case (2)* [1]*. Furthermore, the orthogonal projector onto the noise subspace* $\tilde{\mathbf{\Pi}}_T$ *associated with the sample estimate* $\mathbf{R}_{\tilde{y},T}$ *of* $\mathbf{R}_{\tilde{y}}$ *has the same structure*

$$\tilde{\mathbf{\Pi}}_T = \begin{pmatrix} \mathbf{\Pi}_{1,T} & \mathbf{\Pi}_{2,T} \\ \mathbf{\Pi}_{2,T}^* & \mathbf{\Pi}_{1,T}^* \end{pmatrix} \tag{9.5}$$

where $\mathbf{\Pi}_{1,T}$ *and* $\mathbf{\Pi}_{2,T}$ *are Hermitian and complex symmetric respectively.*

Case (1): Uncorrelated sources with $\rho_k = 1$

Consider now three MUSIC-like algorithms for which (9.4) becomes

$$\mathbf{R}_{\tilde{y}} = \begin{pmatrix} \mathbf{A} \\ \mathbf{A}^* \mathbf{\Delta}_\phi^* \end{pmatrix} \mathbf{\Delta}_\sigma \begin{pmatrix} \mathbf{A} \\ \mathbf{A}^* \mathbf{\Delta}_\phi^* \end{pmatrix}^H + \sigma_n^2 \mathbf{I}_{2M}, \tag{9.6}$$

an algorithm (denoted Alg_1) devised in [3] has been derived from the standard MUSIC algorithm. Specifically, the estimated DOA $(\theta_{k,T})_{k=1,\ldots,K}$ are obtained as the locations of the K smallest minima of the following function:

$$\theta_{k,T}^{\text{Alg}_1} = \arg\min_\theta \left[\min_\phi \tilde{\mathbf{a}}^H(\theta,\phi)\tilde{\mathbf{\Pi}}_T\tilde{\mathbf{a}}(\theta,\phi)\right] = \arg\min_\theta \left(\mathbf{a}^H(\theta)\mathbf{\Pi}_{1,T}\mathbf{a}(\theta) - \left|\mathbf{a}^T(\theta)\mathbf{\Pi}_{2,T}^*\mathbf{a}(\theta)\right|\right), \tag{9.7}$$

with the extended steering vector $\tilde{\mathbf{a}}(\theta,\phi) \stackrel{\text{def}}{=} \begin{pmatrix} \mathbf{a}(\theta) \\ \mathbf{a}^*(\theta)e^{-i\phi} \end{pmatrix}$.

Because $\begin{pmatrix} \mathbf{a}^H(\theta) & e^{i\phi}\mathbf{a}^T(\theta) \end{pmatrix} \tilde{\mathbf{\Pi}} \begin{pmatrix} \mathbf{a}(\theta) \\ \mathbf{a}^*(\theta)e^{-i\phi} \end{pmatrix} = \begin{pmatrix} 1 & e^{i\phi} \end{pmatrix} \mathbf{M} \begin{pmatrix} 1 \\ e^{-i\phi} \end{pmatrix} = 0$ with $\mathbf{M} \stackrel{\text{def}}{=} \begin{pmatrix} \mathbf{a}^H(\theta) & \mathbf{0}^T \\ \mathbf{0}^T & \mathbf{a}^T(\theta) \end{pmatrix} \tilde{\mathbf{\Pi}} \begin{pmatrix} \mathbf{a}(\theta) & \mathbf{0} \\ \mathbf{0} & \mathbf{a}^*(\theta) \end{pmatrix}$, the matrix $\mathbf{M}_T \stackrel{\text{def}}{=} \begin{pmatrix} \mathbf{a}^H(\theta) & \mathbf{0}^T \\ \mathbf{0}^T & \mathbf{a}^T(\theta) \end{pmatrix} \tilde{\mathbf{\Pi}}_T \begin{pmatrix} \mathbf{a}(\theta) & \mathbf{0} \\ \mathbf{0} & \mathbf{a}^*(\theta) \end{pmatrix}$ is positive definite and a consistent estimate of the rank deficient 2×2 matrix $\mathbf{M}$. Using this property, a subspace-based algorithm (denoted Alg_2) is proposed in [10] defined by

$$\theta_{k,T}^{\text{Alg}_2} = \arg\min_\theta g_{2,T}(\theta)$$

with

$$g_{2,T}(\theta) \stackrel{\text{def}}{=} \text{Det}(\mathbf{M}_T) = \left(\mathbf{a}^H(\theta)\mathbf{\Pi}_{1,T}\mathbf{a}(\theta)\right)^2 - \left(\mathbf{a}^T(\theta)\mathbf{\Pi}_{2,T}^*\mathbf{a}(\theta)\right)\left(\mathbf{a}^H(\theta)\mathbf{\Pi}_{2,T}\mathbf{a}^*(\theta)\right). \tag{9.8}$$

In the particular case of a uniform linear array, replacing the generic steering vector $\mathbf{a}(\theta) = (1, e^{i\theta}, \ldots, e^{i(M-1)\theta})^T$ by $\mathbf{a}(z) \stackrel{\text{def}}{=} (1, z, \ldots, z^{M-1})^T$ in (9.8), [4] proposed a root-MUSIC-like algorithm (denoted Alg_3) defined by

$$\theta_{k,T}^{\text{Alg}_3} = \arg(z_k) \;\text{ with } z_k \;\; K \text{ roots}_{|z|<1} \text{ of } \; g_{3,T}(z) \;\text{ closest to the unit circle} \tag{9.9}$$

where $g_{3,T}(z)$ is the following polynomial[2] of degree $4(M-1)$ whose roots appear in reciprocal conjugate pairs z_k and $(z_k^*)^{-1}$:

$$g_{3,T}(z) \stackrel{\text{def}}{=} \left(\mathbf{a}^T(z^{-1})\mathbf{\Pi}_{1,T}\mathbf{a}(z)\right)^2 - \left(\mathbf{a}^T(z)\mathbf{\Pi}_{2,T}^*\mathbf{a}(z)\right)\left(\mathbf{a}^T(z^{-1})\mathbf{\Pi}_{2,T}\mathbf{a}(z^{-1})\right).$$

Considering the performance of these three algorithms, the following is proved in [10]:

[1] We note that $\mathbf{\Pi}_1$ is not a projection matrix in case (1).

[2] We note that this procedure allows one to estimate up to $2(M-1)$ possible DOA.

Theorem 2 *The sequences $\sqrt{T}(\boldsymbol{\theta}_T - \boldsymbol{\theta})$, where $\boldsymbol{\theta}_T$ are the DOA estimates given by these three MUSIC-like algorithms [resp., first two MUSIC-like algorithms] for a uniform linear array [resp., arbitrary array], converge in distribution to the same zero-mean Gaussian distribution[3] of covariance matrix*

$$(\mathbf{C}_{\boldsymbol{\theta}})_{k,l} = \frac{1}{\gamma_k \gamma_l} \begin{pmatrix} \alpha_{\phi,\phi}^{(k)} & -\alpha_{\theta,\phi}^{(k)} \end{pmatrix} \mathbf{B}^{(k,l)} \begin{pmatrix} \alpha_{\phi,\phi}^{(l)} \\ -\alpha_{\theta,\phi}^{(l)} \end{pmatrix} \tag{9.10}$$

with $\left(\mathbf{B}^{(k,l)}\right)_{i,j} \stackrel{\text{def}}{=} 4\Re\left((\tilde{\mathbf{a}}_k^T \tilde{\mathbf{U}}^* \tilde{\mathbf{a}}_l^*)(\tilde{\mathbf{a}'}_{i,k}^H \tilde{\mathbf{\Pi}} \tilde{\mathbf{a}}'_{j,l})\right)$, $i,j = \theta,\phi$ *where* $\tilde{\mathbf{a}}_k \stackrel{\text{def}}{=} \begin{pmatrix} \mathbf{a}_k \\ \mathbf{a}_k^* e^{-i\phi_k} \end{pmatrix}$, $\tilde{\mathbf{a}}'_{\theta,k} \stackrel{\text{def}}{=} \frac{d\tilde{\mathbf{a}}_k}{d\theta_k}$, $\tilde{\mathbf{a}}'_{\phi,k} \stackrel{\text{def}}{=} \frac{d\tilde{\mathbf{a}}_k}{d\phi_k}$, $\tilde{\mathbf{U}} \stackrel{\text{def}}{=} \sigma_n^2 \tilde{\mathbf{S}}^{\#} \mathbf{R}_{\tilde{y}} \tilde{\mathbf{S}}^{\#}$ *with* $\tilde{\mathbf{S}} \stackrel{\text{def}}{=} \tilde{\mathbf{A}} \mathbf{R}_{\tilde{x}} \tilde{\mathbf{A}}^H$, *and with* $\left(\alpha_{i,j}^{(k)}\right)_{i,j=\theta,\phi}$ *and* γ_k *are the purely geometric factors:* $\alpha_{i,j}^{(k)} \stackrel{\text{def}}{=} \Re(\tilde{\mathbf{a}'}_{i,k}^H \tilde{\mathbf{\Pi}} \tilde{\mathbf{a}}'_{j,k})$ *and* $\gamma_k \stackrel{\text{def}}{=} \alpha_{\theta,\theta}^{(k)} \alpha_{\phi,\phi}^{(k)} - (\alpha_{\theta,\phi}^{(k)})^2$. *In particular:*

$$(\mathbf{C}_{\boldsymbol{\theta}})_{k,k} = \frac{2\alpha_{\phi,\phi}^{(k)}}{\gamma_k} (\tilde{\mathbf{a}}_k^H \tilde{\mathbf{U}} \tilde{\mathbf{a}}_k),\ k = 1, \ldots, K \tag{9.11}$$

which gives in the case of a single source:

$$C_{\theta_1} = \frac{1}{\alpha_1 r_1} \left(1 + \frac{1}{2\|\mathbf{a}_1\|^2 r_1}\right). \tag{9.12}$$

Remark: If the case of a single noncircular complex Gaussian distributed source of maximum circularity rate ($\rho_1 = 1$), asymptotic variance (9.12) attains the noncircular Gaussian Cramer-Rao bound (9.23). Consequently, these three MUSIC-like algorithms previously described are efficient for a single source.

Case (2): Arbitrary full rank spatial extended covariance matrix

In that case, based on $\tilde{\mathbf{\Pi}}\tilde{\mathbf{A}} = \begin{pmatrix} \mathbf{\Pi}_1 & \mathbf{\Pi}_2 \\ \mathbf{\Pi}_2^* & \mathbf{\Pi}_1^* \end{pmatrix} \begin{pmatrix} \mathbf{A} & \mathbf{O} \\ \mathbf{O} & \mathbf{A}^* \end{pmatrix} = \mathbf{O}$, different MUSIC-like algorithms can be proposed. Using $\mathbf{\Pi}_2 = \mathbf{O}$, the simplest one[4] (denoted Alg_4) is the following

$$\theta_{k,T}^{\text{Alg}_4} = \arg\min_{\theta} \mathbf{a}^H(\theta) \mathbf{\Pi}_{1,T} \mathbf{a}(\theta). \tag{9.13}$$

Because this algorithm is always outperformed by the standard MUSIC algorithm based on $\mathbf{R}_{y,T}$ only (see [10]), the following column weighting[5] MUSIC (denoted Alg_5) was proposed in [10] by using the ideas of the weighted MUSIC algorithm introduced for DOA estimation [11], then applied for frequency estimation in [12],[13]:

$$\theta_{k,T}^{\text{Alg}_5} = \arg\min_{\theta} g_{5,T}(\theta) \quad \text{with} \quad g_{5,T}(\theta) \stackrel{\text{def}}{=} \text{Tr}\left(\mathbf{W} \bar{\mathbf{A}}^H(\theta) \tilde{\mathbf{\Pi}}_T \bar{\mathbf{A}}(\theta)\right),$$

where $\mathbf{W}$ is a 2×2 non-negative definite weighting matrix, and $\bar{\mathbf{A}}(\theta)$ is the steering matrix $\begin{pmatrix} \mathbf{a}(\theta) & \mathbf{0} \\ \mathbf{0} & \mathbf{a}^*(\theta) \end{pmatrix}$. To derive the optimal weighting matrix $\mathbf{W} = \begin{pmatrix} w_{1,1} & w_{1,2} \\ w_{1,2}^* & w_{2,2} \end{pmatrix}$ in the next section, the weighted MUSIC cost function can be written as

$$g_{5,T}(\theta) = (w_{1,1} + w_{2,2}) \left(\mathbf{a}^H(\theta) \mathbf{\Pi}_{1,T} \mathbf{a}(\theta) + \Re(z \mathbf{a}^T(\theta) \mathbf{\Pi}_{2,T} \mathbf{a}(\theta))\right), \tag{9.14}$$

with $z \stackrel{\text{def}}{=} \frac{2w_{1,2}^*}{w_{1,1}+w_{2,2}}$. Consequently the performance of this algorithm depends only on z. By choosing $\mathbf{W}$ diagonal, we have $z = 0$ and this algorithm reduces to Alg_4. Considering the performance of this algorithm, the following is proved in [10]:

[3] These three algorithms have different behavior outside the asymptotic regime, as will be stressed in Section 9.7.

[4] We note that unlike $\mathbf{\Pi}_1$, $\mathbf{\Pi}_{1,T}$ is not a projection matrix.

[5] Because $\tilde{\mathbf{\Pi}}_T$ is an orthogonal projector, the cost function $g_{5,T}(\theta)$ reduces to $\|\tilde{\mathbf{\Pi}}_T \bar{\mathbf{A}}(\theta) \mathbf{W}^{1/2}\|_{\text{Fro}}^2$.

Theorem 3 *The sequence $\sqrt{T}(\boldsymbol{\theta}_T - \boldsymbol{\theta})$, where $\boldsymbol{\theta}_T$ is the DOA estimate given by this weighted MUSIC algorithm, converges in distribution to the zero-mean Gaussian distribution of covariance matrix*

$$(\mathbf{C}_{\boldsymbol{\theta}})_{k,l} = \frac{1}{2\alpha_k\alpha_l}(1\ z^*\ z\ 1)\left((\bar{\mathbf{A}}_k^T\tilde{\mathbf{U}}^*\bar{\mathbf{A}}_l^*)\otimes(\bar{\mathbf{A}}'^H_k\tilde{\mathbf{\Pi}}\bar{\mathbf{A}}'_l)+(\bar{\mathbf{A}}'^T_k\tilde{\mathbf{\Pi}}^*\bar{\mathbf{A}}'^*_l)\otimes(\bar{\mathbf{A}}_k^H\tilde{\mathbf{U}}\bar{\mathbf{A}}_l)\right)(1\ z^*\ z\ 1)^H, \quad (9.15)$$

with $\bar{\mathbf{A}}_k \overset{\text{def}}{=} \bar{\mathbf{A}}(\theta_k)$ and $\bar{\mathbf{A}}'_k \overset{\text{def}}{=} \frac{d\bar{\mathbf{A}}_k}{d\theta_k}$. Furthermore, the value z_k^{opt} that minimizes $(\mathbf{C}_{\boldsymbol{\theta}})_{k,k}$ is given by

$$z_k^{\text{opt}} = -\frac{\mathbf{a}_k^T\mathbf{U}_2^*\mathbf{a}_k}{\mathbf{a}_k^H\mathbf{U}_1\mathbf{a}_k}, \quad (9.16)$$

with $\tilde{\mathbf{U}} = \begin{pmatrix} \mathbf{U}_1 & \mathbf{U}_2 \\ \mathbf{U}_2^* & \mathbf{U}_1^* \end{pmatrix}$, for which the minimum value of $(\mathbf{C}_{\boldsymbol{\theta}})_{k,k}$ is

$$\min_z (\mathbf{C}_{\boldsymbol{\theta}})_{k,k} = \frac{\text{Det}(\bar{\mathbf{A}}_k^H\tilde{\mathbf{U}}\bar{\mathbf{A}}_k)}{2(\mathbf{a}_k^H\mathbf{U}_1\mathbf{a}_k)(\mathbf{a}'^H_k\mathbf{\Pi}_1\mathbf{a}'_k)}. \quad (9.17)$$

For a single source, we have [10]:

Corollary 1 *The asymptotic variance of the DOA estimate given by this optimal weighting MUSIC algorithm attains the noncircular Gaussian Cramer Rao bound* (9.22) *for all values of the noncircularity rate in the single source case.*

Remark 1: The optimal value of the weight previously derived depends on the specific DOA whose variance is to be minimized, which means that the optimal weight is not the same for all DOAs. This, however, might have been expected as MUSIC estimates the DOAs one by one. In addition, it should be noted that z_k^{opt} is sample dependent. Consequently, this value ought to be replaced by a consistent estimate in the implementation of the optimal weighting MUSIC algorithm. We note that this replacement of z_k^{opt} by a consistent estimate has no effect on the asymptotic variance of the weighting MUSIC algorithm as proved in [10].
Remark 2: For circular sources, $\mathbf{R}_{\tilde{y}}$ is block diagonal. This successively implies that $\tilde{\mathbf{S}}$, $\tilde{\mathbf{S}}^{\#}$ and $\tilde{\mathbf{U}}$ are block diagonal. Consequently, $\mathbf{U}_2 = \mathbf{O}$, $z_k^{\text{opt}} = 0$, $\mathbf{W}_{\text{opt}}$ is diagonal and the optimal weighting MUSIC algorithm reduces to the standard MUSIC algorithm. Then (9.17) becomes $\min_z (\mathbf{C}_{\boldsymbol{\theta}})_{k,k} = \frac{\mathbf{a}_k^H\mathbf{U}\mathbf{a}_k}{2\mathbf{a}'^H_k\mathbf{\Pi}_1\mathbf{a}'_k}$, which is the asymptotic variance given by (9.3).
Remark 3: All the performance results presented until now depend on the distribution of the sources through their second-order moments only. These results can be extended. Following a functional analysis (see [14]) and assuming some regularity conditions, the following is proved in [10, 15]:

Theorem 4 *The asymptotic performance given by an arbitrary subspace-based algorithm built from $\tilde{\mathbf{\Pi}}_T$ [resp. $(\mathbf{\Pi}_T, \mathbf{\Pi}'_T)$] associated with the noise subspace of $\mathbf{R}_{\tilde{y},T}$ [resp. $(\mathbf{R}_{y,T}, \mathbf{R}'_{y,T})$] depends on the distribution of the sources through their second-order moments only.*

Furthermore, using the same approach, it is proved in [10] that the noncircularity of the sources does not change the asymptotic performance of the standard second-order algorithms; more precisely:

Theorem 5 *All DOA consistent estimates given by second-order algorithms based on $\mathbf{R}_{y,T}$ only, that do not suppose explicitly the sources to be spatially uncorrelated, are robust to the distribution and to the noncircularity of the sources; i.e., the asymptotic performances are those of the standard complex circular Gaussian case.*

9.4 Asymptotically minimum variance estimation

To assess the performance and the efficiency of the previous MUSIC-like algorithms, their performances are compared in this section to those of the AMV estimators in the class of consistent estimators based on $\mathbf{R}_{\tilde{y},T}$, i.e., on $(\mathbf{R}_{y,T}, \mathbf{R}'_{y,T})$ [16], then on $(\mathbf{\Pi}_T, \mathbf{\Pi}'_T)$ and on $\tilde{\mathbf{\Pi}}_T$ [15]. Considering the statistic $(\mathbf{R}_{y,T}, \mathbf{R}'_{y,T})$, the following theorem is proved in [15]:

Theorem 6 *The covariance matrix $\mathbf{C}_{\boldsymbol{\alpha}}$ of the asymptotic distribution of an estimator of $\boldsymbol{\alpha}$ given by an arbitrary consistent algorithm based on $(\mathbf{R}_{y,T}, \mathbf{R}'_{y,T})$ is bounded below by the real symmetric matrix $\mathbf{C}_{\boldsymbol{\alpha}}^{\mathrm{AMV(R,R')}} = (\mathcal{S}^H \mathbf{C}_s^{-1}(\boldsymbol{\alpha}) \mathcal{S})^{-1}$*

$$\mathbf{C}_{\boldsymbol{\alpha}} \geq (\mathcal{S}^H \mathbf{C}_s^{-1}(\boldsymbol{\alpha}) \mathcal{S})^{-1} \tag{9.18}$$

where $\mathcal{S} \stackrel{\text{def}}{=} \frac{d\mathbf{s}(\boldsymbol{\alpha})}{d\boldsymbol{\alpha}}$, $\mathbf{s}(\boldsymbol{\alpha}) \stackrel{\text{def}}{=} [\mathrm{vec}^T(\mathbf{R}_y(\boldsymbol{\alpha})), \mathrm{v}^T(\mathbf{R}'_y(\boldsymbol{\alpha})), \mathrm{v}^H(\mathbf{R}'_y(\boldsymbol{\alpha}))]^T$[6] and where $\mathbf{C}_s(\boldsymbol{\alpha})$ is the first covariance matrix of the asymptotic distribution of $\mathbf{s}_T \stackrel{\text{def}}{=} [\mathrm{vec}^T(\mathbf{R}_{y,T}), \mathrm{v}^T(\mathbf{R}'_{y,T}), \mathrm{v}^H(\mathbf{R}'_{y,T})]^T$.

Remark: A priori knowledge on the spatial correlation of the sources may be be introduced in the bound (9.18) by using adapted parameterization of $\mathbf{R}_x$ and $\mathbf{R}'_x$. For example, if the sources are supposed to be spatially uncorrelated, $\mathbf{R}_x$ will be parameterized by $([\mathbf{R}_x]_{k,k})_{k=1,\ldots,K}$ and if, moreover, they are independent, $\mathbf{R}_x$ and $\mathbf{R}'_x$ will be parameterized by $([\mathbf{R}_x]_{k,k}, \Re([\mathbf{R}'_x]_{k,k}), \Im([\mathbf{R}'_x]_{k,k}))_{k=1,\ldots,K}$ only.

Furthermore, it is proved in [15] that this lowest bound is asymptotically tight, i.e., there exists an algorithm whose covariance of the asymptotic distribution of $\boldsymbol{\alpha}_T$ satisfies (9.18) with equality:

Theorem 7 *The following nonlinear least square algorithm is an AMV second-order algorithm:*

$$\boldsymbol{\alpha}_T = \arg \min_{\boldsymbol{\alpha} \in \mathbb{R}^L} [\mathbf{s}_T - \mathbf{s}(\boldsymbol{\alpha})]^H \mathbf{C}_s^{-1}(\boldsymbol{\alpha}) [\mathbf{s}_T - \mathbf{s}(\boldsymbol{\alpha})] \tag{9.19}$$

and this lowest bound (9.18) *is also obtained if an arbitrary consistent estimate $\mathbf{C}_{s,T}$ of $\mathbf{C}_s(\boldsymbol{\alpha})$ is used in* (9.19).

To reduce the computational complexity due to the nonlinear minimization required by this matching approach, the covariance matching estimation techniques (COMET) can be included to simplify this algorithm if the parameterization of $\mathbf{Q}_n$ is linear in $\boldsymbol{\sigma}$ because in this case there exists a matrix $\mathbf{\Psi}(\boldsymbol{\theta})$ such that $\mathbf{s}(\boldsymbol{\alpha}) = \mathbf{\Psi}(\boldsymbol{\theta})(\boldsymbol{\rho}^T, \boldsymbol{\sigma}^T)^T$. Using the approach introduced in [17] and then in [16] with the following consistent estimate $\mathbf{W} \stackrel{\text{def}}{=} \frac{1}{T} \sum_{t=1}^T \left[\left(\mathbf{s}(t) - \frac{1}{T} \sum_{t=1}^T \mathbf{s}(t) \right) \left(\mathbf{s}(t) - \frac{1}{T} \sum_{t=1}^T \mathbf{s}(t) \right)^H \right]$ of $\mathbf{C}_s(\boldsymbol{\alpha})$ where $\mathbf{s}(t) \stackrel{\text{def}}{=} \begin{pmatrix} \mathbf{y}_t^* \otimes \mathbf{y}_t \\ \mathbf{y}_t \otimes \mathbf{y}_t \end{pmatrix}$, the proof given in [16] can be extended, and $\boldsymbol{\theta}_T$ is obtained by

$$\boldsymbol{\theta}_T = \arg \min_{\boldsymbol{\theta} \in \mathbb{R}^K} \mathbf{s}_T^H \mathbf{W} \mathbf{\Psi}(\boldsymbol{\theta}) [\mathbf{\Psi}^H(\boldsymbol{\theta}) \mathbf{W} \mathbf{\Psi}(\boldsymbol{\theta})]^{-1} \mathbf{\Psi}^H(\boldsymbol{\theta}) \mathbf{W} \mathbf{s}_T. \tag{9.20}$$

Furthermore the top left $K \times K$ "DOA corner" of $\mathbf{C}_{\boldsymbol{\alpha}}^{\mathrm{AMV(R,R')}}$ is given by:

$$\mathbf{C}_{\boldsymbol{\theta}}^{\mathrm{AMV(R,R')}} = \left(\mathcal{S}_1^H \mathbf{C}_s^{-1/2}(\boldsymbol{\alpha}) \mathbf{\Pi}^{\perp}_{\mathbf{C}_s^{-1}(\boldsymbol{\alpha})\mathbf{\Psi}} \mathbf{C}_s^{-1/2}(\boldsymbol{\alpha}) \mathcal{S}_1 \right)^{-1}. \tag{9.21}$$

with $\mathcal{S} = [\mathcal{S}_1, \mathbf{\Psi}]$ and where $\mathbf{\Pi}^{\perp}_{\mathbf{C}_s^{-1/2}(\boldsymbol{\alpha})\mathbf{\Psi}}$ denotes the projector onto the orthogonal complement of the columns of $\mathbf{C}_s^{-1/2}(\boldsymbol{\alpha})\mathbf{\Psi}$.

In the particular case where $\mathbf{Q}_n = \sigma_n^2 \mathbf{I}_M$, Theorems 6 and 7 are extended in [15] to the statistics $\mathbf{s}_T = (\mathbf{\Pi}_T, \mathbf{\Pi}'_T)$ and $\mathbf{s}_T = \tilde{\mathbf{\Pi}}_T$ where $\boldsymbol{\theta}$ alone is identifiable from $(\mathbf{\Pi}, \mathbf{\Pi}')$ and $\tilde{\mathbf{\Pi}}$, and where the inverse of the matrix $\mathbf{C}_s$ (which is here singular) is replaced by its Moore Penrose inverse. Furthermore, the following is proved in [18]:

[6] $\mathrm{vec}(\cdot)$ is the "vectorization" operator that turns a matrix into a vector by stacking the columns of the matrix one below another and $\mathrm{v}(.)$ denotes the operator obtained from $\mathrm{vec}(.)$ by eliminating all supradiagonal elements of the matrix.

Theorem 8 *For Gaussian distributed signals, if no a priori information is available on* $\mathbf{R}_x$ *and* $\mathbf{R}'_x$*, the previous different AMV bounds coincide with the normalized*[7] *Gaussian CRB given by Theorem 9 (case (UW)):*

$$\mathbf{C}_{\boldsymbol{\theta}}^{\mathrm{AMV}(\Pi,\Pi')} = \mathbf{C}_{\boldsymbol{\theta}}^{\mathrm{AMV}(\tilde{\Pi})} = \mathbf{C}_{\boldsymbol{\theta}}^{\mathrm{AMV}(\mathrm{R},\mathrm{R}')} = \mathbf{CRB}_{\mathrm{AU}}^{\mathrm{NCG}}(\boldsymbol{\theta}).$$

This proves the efficiency of the AMV estimator based on orthogonal projectors, with respect to CRB. Naturally this result extends to the AMV estimator based on $\mathbf{R}_{y,T}$ only for circular Gaussian signals and explains the good performances of the standard DOA subspace-based algorithms.

9.5 Stochastic Cramer-Rao bound for noncircular Gaussian signals

In this section, the sources are assumed Gaussian distributed. In such a case, expression (9.21) gives the stochastic CRB for the parameter $\boldsymbol{\theta}$ alone. But this expression lacks engineering insight and applies only for a linearly parameterized noise covariance matrix $\mathbf{Q}_n$. Deriving such an interpretable expression for circular Gaussian signals has been an intensive research field. Among them, Stoica and Nehorai [19], Ottersten *et al* [20], Weiss and Friedlander [21] derived this bound indirectly as the asymptotic covariance matrix of the maximum likelihood (ML) estimator for uniform white noise. Ten years later, Stoica *et al* [22], Pesavento and Gershman [23] and Gershman *et al* [8] derived directly this bound from the Slepian-Bangs formula [24, 25] for uniform white, nonuniform white and arbitrary unknown noise field respectively. Using these two approaches, these results are extended in [26] and [9] for noncircular Gaussian sources. The following result is proved in [26] and [9]:

Theorem 9 *The normalized DOA-related block of CRB for noncircular complex Gaussian (NCG) sources in the presence of an arbitrary unknown (AU), nonuniform white (NU) or uniform white (UW) noise field is given by the following explicit expression:*

$$\mathbf{CRB}_{\mathrm{X}}^{\mathrm{NCG}}(\boldsymbol{\theta}) = \frac{1}{2}\left\{\Re\left[\left(\breve{\mathbf{D}}^H\boldsymbol{\Pi}_{\breve{\mathbf{A}}}^{\perp}\breve{\mathbf{D}}\right)\odot\left([\mathbf{R}_s\breve{\mathbf{A}}^H,\mathbf{R}'_s\breve{\mathbf{A}}^T]\bar{\mathbf{R}}_{\tilde{y}}^{-1}\begin{bmatrix}\breve{\mathbf{A}}\mathbf{R}_s\\ \breve{\mathbf{A}}^*\mathbf{R}'^*_s\end{bmatrix}\right)^T\right] - \mathbf{M}_{\mathrm{X}}\mathbf{T}_{\mathrm{X}}^{-1}\mathbf{M}_{\mathrm{X}}^T\right\}^{-1}$$

where $\breve{\mathbf{A}} \overset{\text{def}}{=} \mathbf{Q}_n^{-1/2}\mathbf{A}$, $\breve{\mathbf{D}} \overset{\text{def}}{=} \frac{d\breve{\mathbf{A}}}{d\boldsymbol{\theta}}$, $\bar{\mathbf{R}}_{\tilde{y}} \overset{\text{def}}{=} \mathbf{Q}_{\tilde{n}}^{-1/2}\mathbf{R}_{\tilde{y}}\mathbf{Q}_{\tilde{n}}^{-1/2}$ *with* $\mathbf{Q}_{\tilde{n}} \overset{\text{def}}{=} \begin{pmatrix}\mathbf{Q}_n & \mathbf{O}\\ \mathbf{O} & \mathbf{Q}_n^*\end{pmatrix}$ *and where the expressions of* $\mathbf{M}_{\mathrm{X}}$ *and* $\mathbf{T}_{\mathrm{X}}$ *are given for the* ($\mathrm{X}=\mathrm{AU}$) *and* ($\mathrm{X}=\mathrm{NU}$) *noise field cases in [9] and* $\mathbf{M}_{\mathrm{UW}} = \mathbf{O}$ *and* $\mathbf{T}_{\mathrm{UW}} = \mathbf{O}$ *[26].*

In the particular case of one source, the following is proved in [9]:

Theorem 10 *The normalized CRB of* θ_1 *for a noncircular complex Gaussian source corrupted by nonuniform or uniform white noise field decreases monotonically as the noncircularity rate* ρ_1 *increases and is given by*

$$\mathrm{CRB}_{\mathrm{X}}^{\mathrm{NCG}}(\theta_1) = \frac{1}{\alpha_1}\left[\frac{2r_1^{-1} + \|\mathbf{a}_1\|^{-2}r_1^{-2} + \|\mathbf{a}_1\|^2 - \|\mathbf{a}_1\|^2\rho_1^2}{\|\mathbf{a}_1\|^2 r_1 + 1 + (1-\|\mathbf{a}_1\|^2 r_1)\rho_1^2}\right] \tag{9.22}$$

where the SNR is defined here by $r_1 \overset{\text{def}}{=} \frac{\sigma_{s_1}^2}{M}\sum_{m=1}^{M}\frac{1}{\sigma_m^2}$ *where* $\sigma_m^2 \overset{\text{def}}{=} \mathrm{E}|n_{t,m}^2|$, $m = 1, ..., M$ *and* α_1 *is the noise dependent factor* $2M\left(\sum_{m=1}^{M}\frac{1}{\sigma_m^2}\right)^{-1}\breve{\mathbf{a}}'^H_1\boldsymbol{\Pi}_{\breve{\mathbf{a}}_1}^{\perp}\breve{\mathbf{a}}'_1$ *(*$2\mathbf{a}'^H_1\boldsymbol{\Pi}_{\mathbf{a}_1}^{\perp}\mathbf{a}'_1$ *for uniform white noise) with* $\breve{\mathbf{a}}_1 \overset{\text{def}}{=} \mathbf{Q}_n^{-1/2}\mathbf{a}_1$ *and* $\breve{\mathbf{a}}'_1 \overset{\text{def}}{=} \frac{d\breve{\mathbf{a}}_1}{d\theta_1}$.

Consequently, for one source, the CRB decreases from $\mathrm{CRB}_{\mathrm{NU}}^{\mathrm{CG}}(\theta_1) = \frac{1}{\alpha_1 r_1}\left(1 + \frac{1}{\|\mathbf{a}_1\|^2 r_1}\right)$ ($\rho_1 = 0$, circular case) to

$$\mathrm{CRB}_{\mathrm{NU}}^{\mathrm{NCG}}(\theta_1) = \frac{1}{\alpha_1 r_1}\left(1 + \frac{1}{2\|\mathbf{a}_1\|^2 r_1}\right) \qquad (\rho_1 = 1). \tag{9.23}$$

[7] (i.e., for $T = 1$ throughout this chapter).

Furthermore, this bound has also been compared to the CRB for circular Gaussian sources and to the deterministic CRB in [9], where the following results are proved

Theorem 11 *The DOA-related block of CRB for noncircular complex Gaussian sources is upper bounded by the associated CRB for circular complex Gaussian sources corresponding to the same first covariance matrix* $\mathbf{R}_s$ *and the same arbitrary noise covariance matrix* $\mathbf{Q}_n$*.*

$$\mathbf{CRB}_{Q_n}^{\mathrm{NCG}}(\boldsymbol{\theta}) \leq \mathbf{CRB}_{Q_n}^{\mathrm{CG}}(\boldsymbol{\theta}).$$

Compared to the asymptotic deterministic CRB: $\mathbf{CRB}_{Q_n}^{\mathrm{DET}}(\boldsymbol{\theta}) = \frac{1}{2}\left\{\Re\left[(\breve{\mathbf{D}}^H \boldsymbol{\Pi}_{\breve{\mathbf{A}}}^{\perp} \breve{\mathbf{D}}) \odot \mathbf{R}_s^T\right]\right\}^{-1}$ *which is unchanged with respect to the circular case,*

$$\mathbf{CRB}_{Q_n}^{\mathrm{DET}}(\boldsymbol{\theta}) \leq \mathbf{CRB}_{Q_n}^{\mathrm{NCG}}(\boldsymbol{\theta}).$$

This result proves that for noncircular sources, a potential performance improvement of any second-order algorithm can be expected with respect to a second-order algorithms based on the standard covariance only. Furthermore, compared to the circular case, the deterministic CRB approaches the stochastic noncircular Gaussian CRB.

9.6 Stochastic Cramer-Rao bound for BPSK signals

In the case of noncircular discrete distributed sources, the stochastic CRB appears to be prohibitive to compute. However, for independent BPSK modulated sources in uniform or nonuniform white noise field with $\|\mathbf{a}(\theta)\|^2 = M$, interpretable closed-form expressions of the stochastic CRB can be derived. Compared to those associated with QPSK modulated sources, it is proved in [27] for uniform white noise, then extended to nonuniform white noise in [28] by simple whitening of the noise covariance matrix with $\boldsymbol{\alpha} = (\theta_1, \phi_1, \sigma_{s_1}, \boldsymbol{\sigma}^T)^T$.

Theorem 12 *For a single BPSK or QPSK modulated source, the normalized stochastic CRB of the DOA alone are given by the closed-form expressions*

$$\mathrm{CRB}_{\mathrm{NU}}^{\mathrm{BPSK}}(\theta_1) = \frac{1}{\alpha_1 r_1}\left(\frac{1}{1-f(Mr_1)}\right) \qquad \mathrm{CRB}_{\mathrm{NU}}^{\mathrm{QPSK}}(\theta_1) = \frac{1}{\alpha_1 r_1}\left(\frac{1}{1-f(\frac{Mr_1}{2})}\right)$$

where α_1 *and* r_1 *are given in Theorem 10 and with* $f(\rho)$ *is the following decreasing function of* ρ*:* $f(\rho) \stackrel{\mathrm{def}}{=} \frac{e^{-\rho}}{\sqrt{2\pi}} \int_{-\infty}^{+\infty} \frac{e^{-\frac{u^2}{2}}}{\cosh(u\sqrt{2\rho})} du$*.*

We note that $\mathrm{CRB}_{\mathrm{NU}}^{\mathrm{BPSK}}(\theta_1) < \mathrm{CRB}_{\mathrm{NU}}^{\mathrm{QPSK}}(\theta_1)$ and that compared to the stochastic complex Gaussian CRB (see Theorem 10) associated with the same noncircularity rate (1 and 0 for a BPSK and QPSK modulated source respectively):

$$\frac{\mathrm{CRB}_{\mathrm{NU}}^{\mathrm{BPSK}}(\theta_1)}{\mathrm{CRB}_{\mathrm{NU}}^{\mathrm{NCG}}(\theta_1)} = \frac{1}{(1-f(Mr_1))(1+\frac{1}{2Mr_1})} \quad \text{and} \quad \frac{\mathrm{CRB}_{\mathrm{NU}}^{\mathrm{QPSK}}(\theta_1)}{\mathrm{CRB}_{\mathrm{NU}}^{\mathrm{CG}}(\theta_1)} = \frac{1}{(1-f(\frac{Mr_1}{2}))(1+\frac{1}{Mr_1})}.$$

We note that these ratios depend on Mr_1 only and tend to 1 when Mr_1 tends to ∞.

For two independent BPSK or QPSK modulated sources, we prove [27, 28] that for large SNRs (i.e., $\sum_{m=1}^{M} \frac{\sigma_{s_1}^2}{\sigma_m^2} \gg 1$ and $\sum_{m=1}^{M} \frac{\sigma_{s_2}^2}{\sigma_m^2} \gg 1$) *the CRB for the DOA of one source is independent of the parameters of the other source* and

$$\mathrm{CRB}_{\mathrm{NU}}^{\mathrm{BPSK}}(\theta_1, \theta_2) \approx \mathrm{CRB}_{\mathrm{NU}}^{\mathrm{QPSK}}(\theta_1, \theta_2) \approx \begin{bmatrix} \frac{1}{\alpha_1 r_1} & 0 \\ 0 & \frac{1}{\alpha_2 r_2} \end{bmatrix} \tag{9.24}$$

We note that this property is quite different from the behavior of the CRB under the circular Gaussian distribution and the deterministic CRB, for which the normalized CRB for the DOA of one source depends on the DOA separation. More precisely, it is proved [19, result R9] that these latter two CRBs tend to the same limit as all SNRs increase. For independent sources, they are given by (from, e.g., [19, rel. (2.13)])

$$\mathrm{CRB}_{\mathrm{UW}}^{\mathrm{DET}}(\theta_1,\theta_2) = \mathrm{CRB}_{\mathrm{UW}}^{\mathrm{CG}}(\theta_1,\theta_2) = \begin{bmatrix} \frac{1}{\beta_1 r_1} & 0 \\ 0 & \frac{1}{\beta_2 r_2} \end{bmatrix} \quad \text{with} \quad \beta_k \stackrel{\text{def}}{=} 2\left(\|\mathbf{a}_k'\|^2 - \gamma_k(\theta_1,\theta_2)\right),\ k=1,2,$$

where $\gamma_k(\theta_1,\theta_2), k=1,2$ depends on the source separation. This strange property of the stochastic CRB for independent BPSK sources is illustrated in the next section with the performance of the EM algorithm.

As a consequence, the behavior of the resolution threshold for two equipowered ($r \stackrel{\text{def}}{=} r_1 = r_2$ et $\alpha \stackrel{\text{def}}{=} \alpha_1 = \alpha_2$) closely spaced independent sources is also quite different. Despite the CRB does not directly indicate the best resolution achievable by an unbiased estimator, it can be used to define an absolute limit of resolution. Following the criterium described in [29], two sources are meaningfully resolved if the root mean square of the CRB of the estimated DOA separation $(\theta_{1,T} - \theta_{2,T})$ is less than the DOA separation, i.e.,

$$\sqrt{\mathrm{CRB}_{\mathrm{PSK}}(\theta_1-\theta_2)} = \sqrt{\frac{2}{T}\frac{1}{\alpha r}} < \Delta\theta,$$

because θ_1 and θ_2 are decoupled in (9.24). This resolution bounds the resolution of all unbiased DOA estimates in the regimes SNR $\gg 1$, where the CRB holds. For a ULA, $\alpha r = 2\sigma^2[\sum_{m=1}^{M-1}\frac{m^2}{\sigma_m^2} - (\sum_{m=1}^{M-1}\frac{m}{\sigma_m^2})^2(\sum_{m=1}^{M}\frac{1}{\sigma_m^2})^{-1}]$ which is an extended SNR r_e ($r_e = \frac{M(M^2-1)}{6}\frac{\sigma^2}{\sigma_n^2}$ for the specific case of uniform white noise) and we get:

$$r_e > \frac{2}{T(\Delta\theta)^2} \ \text{ and } \ \frac{\sigma^2}{\sigma_n^2} > \frac{12}{TM(M^2-1)(\Delta\theta)^2} \ \text{ for uniform white noise,}$$

which compared to Gaussian distributed sources for which the SNR threshold varies as $(\Delta\theta)^{-4}$ or $(\Delta\theta)^{-3}$ according to the domain of T (see [30, (35)] for the MUSIC algorithm which is asymptotically efficient as the SNR tends to infinity) is quite different.

9.7 Illustrative examples

In this section, we provide numerical illustrations and Monte Carlo simulations of the performance of the different algorithms presented in Section 9.3, numerical comparisons of the variances of these DOA estimates to the asymptotic variance of AMV estimators based on $\mathbf{R}_{\tilde{y},T}$ (i.e., $\mathbf{R}_{y,T}$ and $\mathbf{R}'_{y,T}$) and on $\mathbf{R}_{y,T}$ alone [16] and numerical illustrations of the AMV bounds and of the CRBs given in Sections 9.5 and 9.6, respectively. Finally Monte Carlo simulations of the EM algorithm illustrate some strange properties presented in Section 9.6.

We consider throughout this section two equipowered ($\sigma^2 \stackrel{\text{def}}{=} \sigma_{s_1}^2 = \sigma_{s_2}^2$) filtered or unfiltered BPSK modulated signals with identical noncircularity rate ($\rho_{nc} \stackrel{\text{def}}{=} \rho_1 = \rho_2$) with phases of circularity ϕ_1 and ϕ_2. These signals consist of two equipowered multipaths issued from the DOAs θ_1 and θ_2. Referenced on the first sensor and from the DOA θ_1, we have equivalently: $x_{t,1} = \bar{x}_{t,1}$ and $x_{t,2} = \cos(\alpha)\bar{x}_{t,1} + \sin(\alpha)\bar{x}_{t,2}$ with $\mathbf{R}_{\bar{x}} = \sigma^2\mathbf{I}_2$ and $\mathbf{R}'_{\bar{x}} = \sigma^2\rho_{nc}\begin{pmatrix} e^{i\phi_1} & 0 \\ 0 & e^{i\phi_2} \end{pmatrix}$. Consequently,

$$\mathbf{R}_x = \sigma^2\begin{pmatrix} 1 & \cos(\alpha) \\ \cos(\alpha) & 1 \end{pmatrix} \quad \text{and} \quad \mathbf{R}'_x = \sigma^2\rho_{nc}\begin{pmatrix} e^{i\phi_1} & \cos(\alpha)e^{i\phi_1} \\ \cos(\alpha)e^{2i\phi_1} & \cos^2(\alpha)e^{i\phi_1} + \sin^2(\alpha)e^{i\phi_2} \end{pmatrix}.$$

These signals impinge on a uniform linear array with $M = 6$ sensors separated by a half-wavelength for which $\mathbf{a}_k = (1, e^{i\theta_k}, \ldots, e^{i(M-1)\theta_k})^T$ where $\theta_k = \pi \sin(\psi_k)$, with ψ_k the DOAs relative to the normal of the array. 1000 independent simulation runs have been performed to obtain the estimated variances and the number of independent snapshots is $T = 500$ (unless explicitly stated otherwise).

The first experiment illustrates Theorem 2 for which $\rho_{nc} = 1$ and $\alpha = \pi/2$. Figs.9.1, 9.2 and 9.3 exhibit the dependence of $\mathrm{var}(\theta_{1,T})$ given by algorithms 1, 2 and 3, and by the AMV algorithm based on $\mathbf{R}_{\tilde{y},T}$ (i.e., on $\mathbf{R}_{y,T}$ and $\mathbf{R}'_{y,T}$), with the SNR, the DOA separation $\Delta\theta = \theta_2 - \theta_1$ and the circularity phase separation $\Delta\phi = \phi_2 - \phi_1$ [8]. Figs.9.1 and 9.2 shows that the domain of validity of our asymptotic analysis depends on the algorithm. Below a SNR threshold that is algorithm-dependent, algorithm 3 (root-MUSIC-like algorithm) outperforms algorithm 2 which outperforms algorithm 1, and naturally all three algorithms clearly outperform the standard MUSIC and the AMV algorithm based on $\mathbf{R}_{y,T}$ alone. In Fig.9.2, we note that the asymptotic variances given by algorithms 1, 2 and 3 and the AMV algorithm tend to a finite limit when the DOA separation decreases to zero. For algorithms 1, 2 and 3, this strange behavior is explained by the two non-zero eigenvalues $(\lambda_k)_{k=1,2}$ of $\tilde{\mathbf{S}}$ which interact in $\tilde{\mathbf{U}} \stackrel{\mathrm{def}}{=} \sigma_n^2 \tilde{\mathbf{S}}^{\#} \mathbf{R}_{\tilde{y}} \tilde{\mathbf{S}}^{\#}$ given in rel. (9.11) of Theorem 2. With $\lambda_k = 2M\sigma_{s_1}^2 \left(1 + (-1)^k \cos((M-1)\frac{\Delta\theta}{2} - \Delta\phi) \frac{\sin(M\frac{\Delta\theta}{2})}{M \sin(\frac{\Delta\theta}{2})}\right)$ $k = 1, 2$, we see that one of these eigenvalues approaches zero and consequently the asymptotic variances increase without limit *only if both* $\Delta\theta$ and $\Delta\phi$ tend to zero. For the AMV algorithm, $\mathbf{C}_{\boldsymbol{\theta}} = \left[(\mathcal{S}^H \mathbf{C}_s^{\#} \mathcal{S})^{-1}\right]_{(1:K,1:K)}$ and $\mathcal{S}$ is column rank deficient *only if both* $\Delta\theta$ and $\Delta\phi$ tend to zero as well. Fig.9.3 illustrates the sensitivity of the performance to the circularity phase separation $\Delta\phi$, which is particularly prominent for low DOA separations. Figs.9.1 and 9.2 show the favorable efficiency of these three algorithms compared to the AMV estimator based on $\mathbf{R}_{\tilde{y},T}$, particularly for large DOA separations. To specify this point, Fig.9.4 exhibits the ratio $r_1 \stackrel{\mathrm{def}}{=} \mathrm{Var}_{\theta_1}^{\mathrm{AMV(R,R')}} / \mathrm{Var}_{\theta_1}^{\mathrm{Alg}_{1,2,3}}$ as a function of the SNR for different DOA separations. It shows that algorithms 1, 2 and 3 are very efficient, except for low DOA separations and low SNRs.

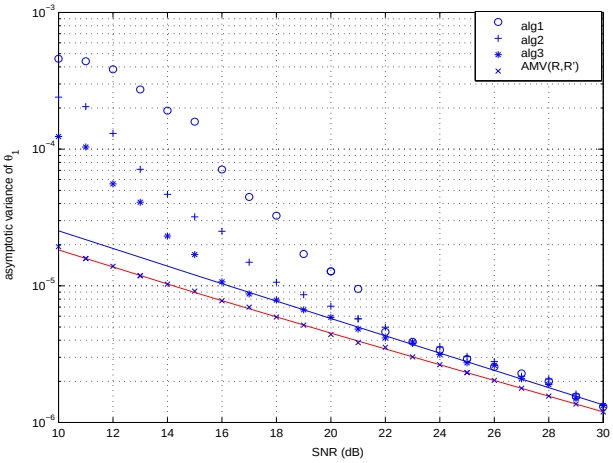

Fig.9.1 Theoretical (solid line) and empirical asymptotic variances given by algorithms 1, 2, 3 and AMV algorithms based on $(\mathbf{R}_{y,T}, \mathbf{R}'_{y,T})$ as a function of the SNR for $\Delta\theta = 0.05$rd, $\Delta\phi = \pi/6$rd.

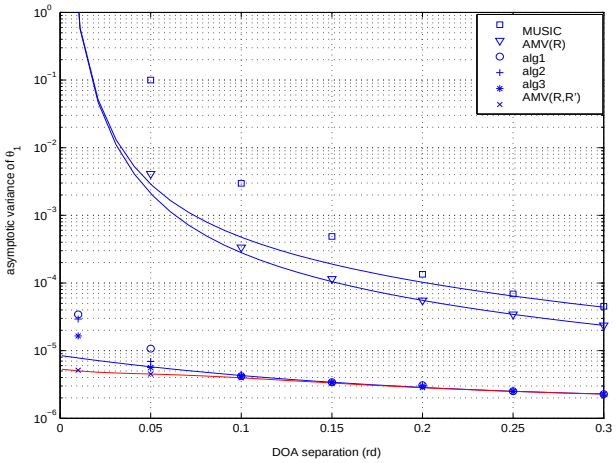

Fig.9.2 Theoretical (solid line) and empirical asymptotic variances given by algorithms 1, 2, 3, standard MUSIC and AMV algorithm based on $\mathbf{R}_{y,T}$ only and on $(\mathbf{R}_{y,T}, \mathbf{R}'_{y,T})$ as a function of the DOA separation for SNR=$20dB$, $\Delta\phi = \pi/6$rd.

[8] Note that one finds, by numerical examples, for two equipowered sources with identical noncircularity rates, that the different theoretical variances depend on θ_1, θ_2, ϕ_1, ϕ_2 by only $\Delta\theta = \theta_2 - \theta_1$ and $\Delta\phi = \phi_2 - \phi_1$ in case (1) [only $\Delta\theta = \theta_2 - \theta_1$ in case (2)] .

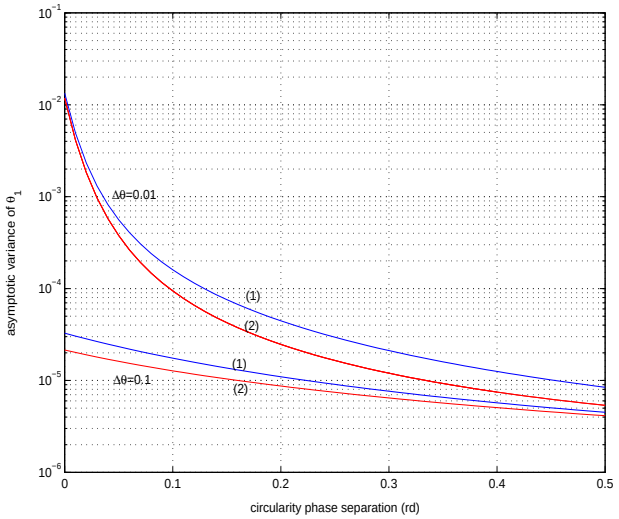

Fig.9.3 Theoretical asymptotic variances given by algorithms 1, 2, 3 (1) and by the AMV algorithm based on $(\mathbf{R}_{y,T}, \mathbf{R}'_{y,T})$ (2) as a function of the circularity phase separation for two DOA separations and SNR=20dB.

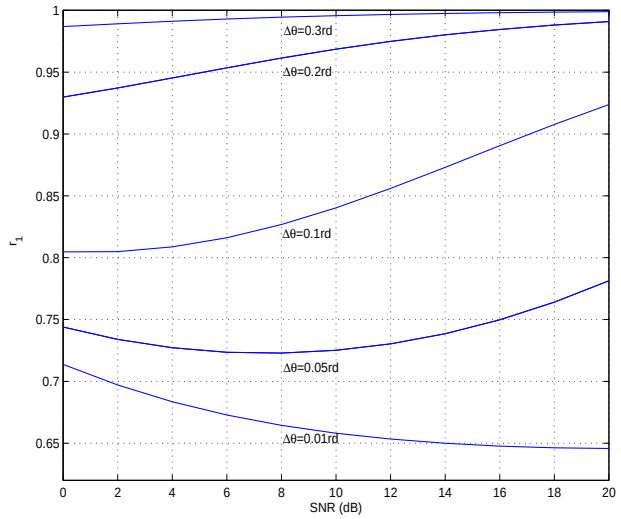

Fig.9.4 Ratio $r_1 \overset{\text{def}}{=} \text{Var}_{\theta_1}^{\text{AMV(R,R}')}/\text{Var}_{\theta_1}^{\text{Alg}_{1,2,3}}$ as a function of the SNR for different DOA separations, $\Delta\phi = \pi/6$rd.

The second experiment illustrates Theorem 3. The noncircularity rate ρ_{nc} is arbitrary and $\alpha = \pi/2$. Compared to the standard MUSIC algorithm based on $\mathbf{R}_{y,T}$, Figs.9.5 and 9.6 shows that algorithm 5 outperforms this MUSIC algorithm, particularly for low SNRs and DOA separations when the circularity rate ρ increases.

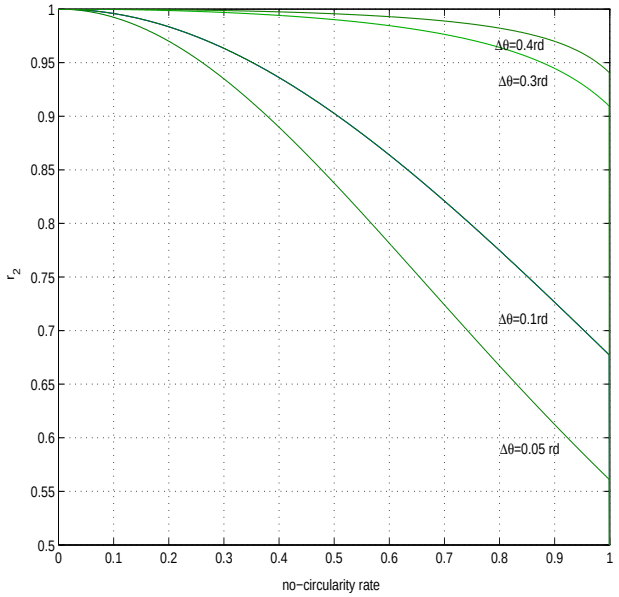

Fig.9.5 Ratio $r_2 \overset{\text{def}}{=} \text{Var}_{\theta_1}^{\text{Alg}_5}/\text{Var}_{\theta_1}^{\text{MUSIC(R)}}$ as a function of the noncircularity rate for different DOA separations for SNR=5dB.

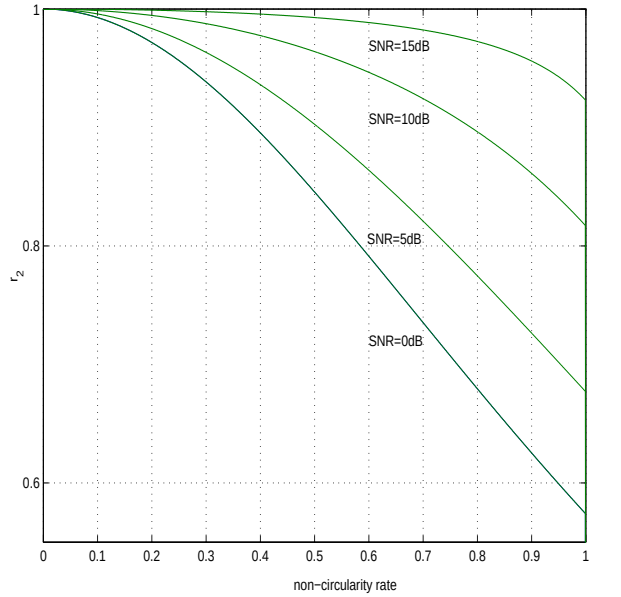

Fig.9.6 Ratio $r_2 \overset{\text{def}}{=} \text{Var}_{\theta_1}^{\text{Alg}_5}/\text{Var}_{\theta_1}^{\text{MUSIC(R)}}$ as a function of the noncircularity rate for different SNRs for $\Delta\theta = 0.1$rd.

To implement the optimal weighted MUSIC algorithm, the following multistep procedure described in [13, Section 7] has been proposed in [10]:

1. Determine standard MUSIC estimates of $(\theta_k)_{k=1,...,K}$ from $\mathbf{R}_{y,T}$.

2. For $k = 1, ..., K$, perform the following: Let $\theta^0_{k,T}$ denote the estimates obtained in step 1. Use $(\theta^0_{k,T})_{k=1,...,K}$ and the estimate $\mathbf{U}_{1,T}$ and $\mathbf{U}_{2,T}$ of $\mathbf{U}_1$ and $\mathbf{U}_2$ derived from $\tilde{\mathbf{R}}_{y,T}$ to obtain consistent

estimates $z_{k,T}$ of z_k^{opt}. Then determine improved estimates $\theta_{k,T}^1$ by locally minimizing the weighted MUSIC cost function (9.13) associated with $z_{k,T}$ around $\theta_{k,T}^0$.

The following table compares our theoretical asymptotic variance expressions with empirical mean square errors (MSEs) obtained from Monte Carlo simulations for the standard MUSIC and the optimal weighted MUSIC algorithms for $\rho = 0.9$, $\Delta\theta = 0.2$rd. We see that there is an agreement between the theoretical and empirical results beyond a SNR threshold. Below this threshold, the optimal weighted MUSIC algorithm largely outperforms the standard MUSIC algorithm.

	Standard MUSIC		Optimal weighted MUSIC	
SNR(dB)	empirical MSE	theoretical variance	empirical MSE	theoretical variance
6	$4.452.10^{-3}$	$4.589.10^{-4}$	$3.154.10^{-4}$	$4.151.10^{-4}$
8	$1.600.10^{-3}$	$2.604.10^{-4}$	$2.344.10^{-4}$	$2.449.10^{-4}$
10	$2.899.10^{-4}$	$1.527.10^{-4}$	$1.561.10^{-4}$	$1.474.10^{-4}$
20	$1.338.10^{-5}$	$1.348.10^{-5}$	$1.337.10^{-5}$	$1.347.10^{-5}$

The third experiment exhibits the benefits due to the second covariance matrix $\mathbf{R}'_{y,T}$ through the comparisons between the AMV bounds based on $(\mathbf{R}_{y,T}, \mathbf{R}'_{y,T})$ and those based on $\mathbf{R}_{y,T}$ only. Figs.9.7 and 9.8 show the ratio $var_{\theta_1}^{\text{AMV(R,R}')}/var_{\theta_1}^{\text{AMV(R)}}$ as a function of the noncircularity rate for $\alpha = \pi/2$rd [resp. $\Delta\theta = 0.1$rd] fixed for different values of $\Delta\theta$ [resp. α] when no a priori information is taken into account. We see that for large DOA separations and/or large spatial correlation between the sources, the second covariance matrix contributes almost no additional information beyond the information in the first covariance matrix. If this spatial uncorrelation a priori information ($\alpha = \pi/2$rd) is taken into account, Fig.9.9 shows the anticipated benefits due to the noncircularity, particularly for low DOA separations. Consequently, the subspace-based algorithms lose their efficiency in these circumstances.

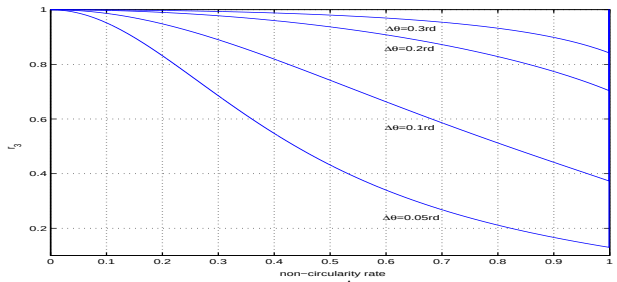

Fig.9.7 Ratio $r_3 \overset{\text{def}}{=} var_{\theta_1}^{\text{AMV(R,R}')}/var_{\theta_1}^{\text{AMV(R)}}$ as a function of the noncircularity rate for different DOA separations for SNR=$5dB$, $\alpha = \pi/2$rd and $\Delta\phi = \pi/6$rd.

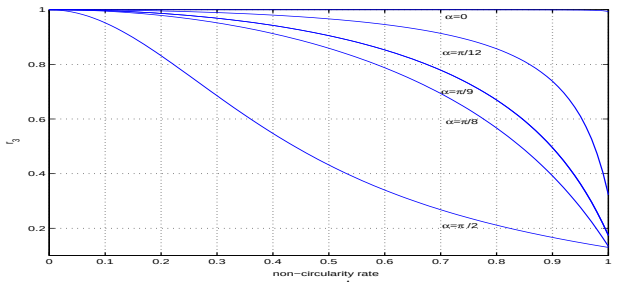

Fig.9.8 Ratio $r_3 \overset{\text{def}}{=} var_{\theta_1}^{\text{AMV(R,R}')}/var_{\theta_1}^{\text{AMV(R)}}$ as a function of the noncircularity rate for different spatial correlation α for SNR=$5dB$, $\Delta\theta = 0.1$rd and $\Delta\phi = \pi/6$rd.

The fourth experiment considers a non white noise field modelled by the two following covariance matrices $\mathbf{Q}_n^{(1)}(k,l) = \sigma_n^2 \exp(-(k-l)^2\zeta)$ and $\mathbf{Q}_n^{(2)}(k,l) = \sigma_n^2 \exp(-|k-l|\zeta)$ introduced in [8]. In these noise field models, $\boldsymbol{\sigma}^T = (\sigma_n^2, \zeta)$ where ζ is the 'color' parameter and the SNR is defined by $\frac{\sigma_{s_1}^2}{\sigma_n^2}$. Fig.9.10 shows the bounds $\text{CRB}_{\text{AU}}^{\text{NCG}}(\theta_1)$, $\text{CRB}_{\text{AU}}^{\text{CG}}(\theta_1)$ and $\text{CRB}_{\text{AU}}^{\text{DET}}(\theta_1)$ [9] plotted against ζ for $\Delta\theta = \theta_2 - \theta_1 = 0.1rd$ and $SNR = 0$dB. We note that when ζ decreases all the CRBs approach zero because $\mathbf{Q}_n$ becomes singular. When $\zeta \gg 1$, the two noise models tend to a uniform white noise model and the two CRBs associated with the models merge. We see that the stochastic CRB under noncircular complex Gaussian distributed sources is visibly larger than the deterministic CRB.

[9] Note that you find by simulation that the different CRBs depend on θ_1, θ_2, ϕ_1, ϕ_2 by only $\Delta\theta = \theta_2 - \theta_1$ and $\Delta\phi = \phi_2 - \phi_1$ for two equipowered sources with identical noncircularity rates.

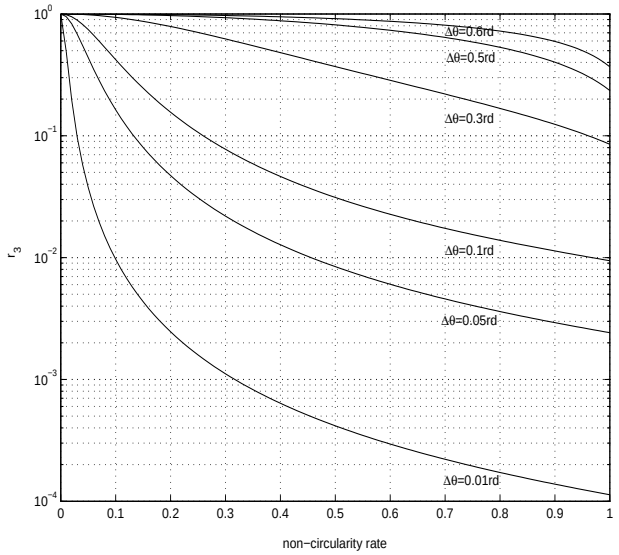

Fig.9.9 Ratio $r_3 \stackrel{\text{def}}{=} var_{\theta_1}^{\text{AMV(R,R')}}/var_{\theta_1}^{\text{AMV(R)}}$ as a function of the noncircularity rate for different DOA separations for SNR=$5dB$. $\Delta\phi = \pi/6$rd.

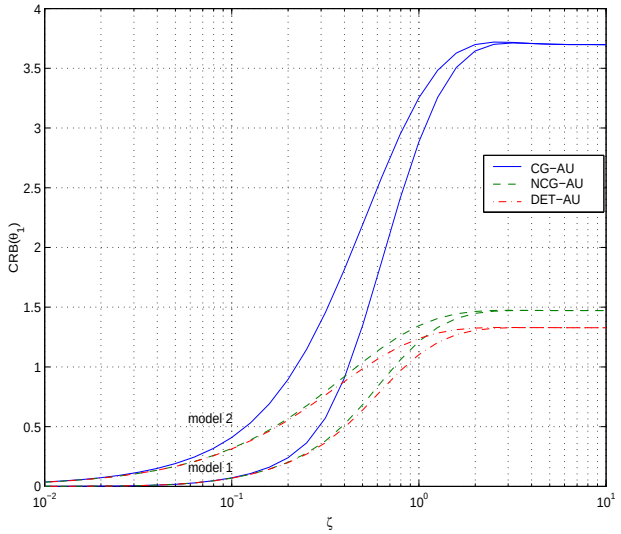

Fig.9.10 $\text{CRB}_{\text{AU}}^{\text{NCG}}(\theta_1)$, $\text{CRB}_{\text{AU}}^{\text{CG}}(\theta_1)$ and $\text{CRB}_{\text{AU}}^{\text{DET}}(\theta_1)$ as a function of ζ for the first and second models with $\Delta\theta = 0.2rd$, SNR= $0dB$ and $\Delta\phi = \pi/6$rd.

The last experiment illustrates the stochastic CRB for BPSK sources for uniform white noise. Fig.9.11 shows the ratios $\frac{\text{CRB}_{\text{BPSK}}(\theta_1)}{\text{CRB}_{\text{NCG}}(\theta_1)}$ and $\frac{\text{CRB}_{\text{QPSK}}(\theta_1)}{\text{CRB}_{\text{CG}}(\theta_1)}$ as a function of $\rho \stackrel{\text{def}}{=} Mr_1$ for a single source. We see from that figure that the CRB's under the noncircular [resp., circular] complex Gaussian distribution are tight upper bounds on the CRB's under the BPSK [resp., QPSK] distribution at very low and very high SNRs only. The last three figures are devoted to two BPSK independent sources and uniform white noise. Fig.9.12 exhibits the domain of validity of the high SNR approximation[10]. We see from this figure that this domain depends not only on M, SNR and DOA separation, but also on the distributed sources. It is shown that this domain reduces for QPSK sources compared to BPSK sources. The larger the DOA separation is or the larger M is, the larger the domain of validity of the approximation is.

Since the CRB under the noncircular [resp., circular] Gaussian distribution is a very loose upper bound on the CRB under the discrete BPSK [resp., QPSK] distribution, specifically for small DOA or phase separation, the ML estimators that take these discrete distributions into account outperform the stochastic ML estimator under the circular Gaussian distribution (see e.g., [19]) and the weighted subspace fitting estimator (see e.g., [20]) which both reach $\text{CRB}_{\text{CG}}(\theta_1)$. Consequently, the EM approaches [31] that are iterative procedures capable of implementing the stochastic ML estimator under these discrete distributions outperform the ML estimator under noncircular or circular Gaussian distribution.

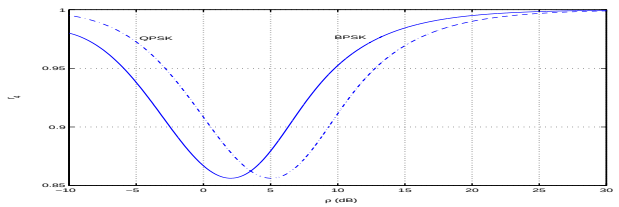

Fig.9.11 Ratios $r_4 \stackrel{\text{def}}{=} \frac{\text{CRB}_{\text{BPSK}}(\theta_1)}{\text{CRB}_{\text{NCG}}(\theta_1)}$ and $r_1(\theta_1) \stackrel{\text{def}}{=} \frac{\text{CRB}_{\text{QPSK}}(\theta_1)}{\text{CRB}_{\text{CG}}(\theta_1)}$ as a function of $\rho \stackrel{\text{def}}{=} Mr_1$.

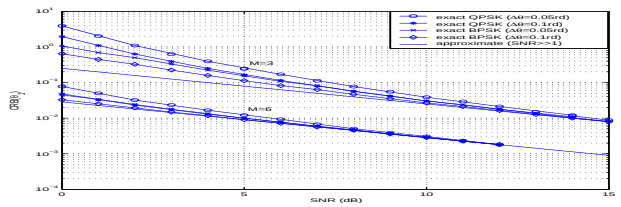

Fig.9.12 Approximate and exact value of $\text{CRB}_{\text{BPSK}}(\theta_1)$ and $\text{CRB}_{\text{QPSK}}(\theta_1)$ as a function of the SNR for different values of the DOA separation.

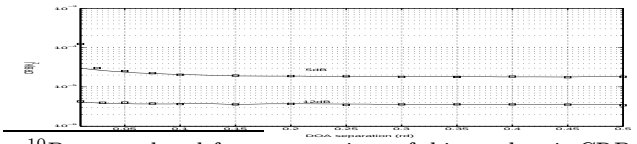

Fig.9.13 $\text{CRB}_{\text{BPSK}}(\theta_1)$ and estimated MSE $\text{E}(\theta_{1,T} - \theta_1)^2$ given by the deterministic EM algorithm (10 iterations) as a function of the DOA separation for $\Delta\phi = 0.1$rd.

[10] Because closed-form expressions of this stochastic CRB appears to be prohibitive to compute, a numerical approximation of the Fisher information matrix derived from the strong law of large numbers is used as a reference.

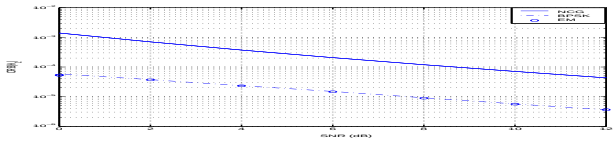

Fig.9.14 $\mathrm{CRB}_{\mathrm{BPSK}}(\theta_1)$, $\mathrm{CRB}_{\mathrm{NCG}}(\theta_1)$ and estimated MSE $\mathrm{E}(\theta_{1,T}-\theta_1)^2$ given by the deterministic EM algorithm (5 iterations), for $\Delta\theta = 0.3rd$ and $\Delta\phi = 0.1$rd, versus SNR.

Fig.9.13 exhibits $\mathrm{CRB}_{\mathrm{BPSK}}(\theta_1)$ and the estimated mean square error (MSE) $\mathrm{E}(\theta_{1,T}-\theta_1)^2$ given by the deterministic EM algorithm initialized by the estimate given by MUSIC-like algorithm 1 described in Section 9.3, as a function of the DOA separation for two SNR's. We see that contrary to $\mathrm{CRB}_{\mathrm{NCG}}(\theta_1)$ (see Figs.9.7 and 9.9), $\mathrm{CRB}_{\mathrm{BPSK}}(\theta_1)$ does not increase significantly when decreasing the DOA separation. Fig.9.14 compares the MSE $\mathrm{E}(\theta_{1,T}-\theta_1)^2$ given by the deterministic EM algorithm (initialized as in Fig.9.13) to $\mathrm{CRB}_{\mathrm{BPSK}}(\theta_1)$ and $\mathrm{CRB}_{\mathrm{NCG}}(\theta_1)$, as a function of the SNR. We see from this figure, that the EM estimate reaches $\mathrm{CRB}_{\mathrm{BPSK}}(\theta_1)$ which largely outperforms $\mathrm{CRB}_{\mathrm{NCG}}(\theta_1)$.

9.8 Conclusion

This chapter has presented an overview of DOA estimation for noncircular signals by considering algorithms and performance bounds. From the viewpoint of algorithms, we have proved that three specific MUSIC-like algorithms built under uncorrelated sources with maximum noncircularity rate, largely outperform the standard MUSIC algorithm. In the general case of nonsingular extended spatial covariance of the sources, the optimal weighted MUSIC that we have introduced outperforms the standard MUSIC algorithm as well, but the performance gain is prominent for low SNRs and DOA separations only. Furthermore, this optimal weighted MUSIC is computationally more demanding than the standard MUSIC algorithm. Consequently, from an application viewpoint, this performance gain might not justify the extra computational load. In this general case, only a multidimensional non-linear optimization algorithm such as the AMV estimator is able to totally benefit from the noncircular property. From the viewpoint of performance bounds, through the stochastic Gaussian CRBs and the AMV bounds, it is proved that the benefits due to the second covariance matrix occurs primarily for low SNRs and DOA separations, particularly when the sources are uncorrelated with maximum noncircularity rates if this a priori knowledge is taken into account. In the specific case of BPSK modulated sources, it is proved that the stochastic CRB for the DOA of one source is independent of the parameters of the other source over wide SNR ranges. Consequently, ML implementations such as the EM approaches outperform the ML estimator under the circular Gaussian distribution, especially for small DOA or phase separations.

References

[1] L.C. Godara, "Application of antenna arrays to mobile communications, Part II: beamforming and direction of arrival considerations," *Proceedings of the IEEE*, vol. 85, pp. 1193-1245, August 1997.

[2] B. Picinbono, "On circularity," *IEEE Trans. Signal Processing*, vol. 42, no. 12, pp. 3473-3482, December 1994.

[3] P. Gounon, C. Adnet and J. Galy, "Angular location for noncircular signals," *Traitement du Signal*, vol. 15, no. 1 pp. 17-23, 1998.

[4] P. Chargé, Y. Wang and J. Saillard, "A noncircular sources direction finding method using polynomial rooting," *Signal Processing*, vol. 81, pp. 1765-1770, 2001.

[5] O. Grellier, P. Comon, B. Mourrain and P. Trebuchet, "Analytical blind channel identification," *IEEE Trans. on Signal Processing*, vol. 50, no. 9, pp. 2196-2207, September 2002.

[6] P. Stoica, R. Moses, "Introduction to spectral analysis," *Prentice-Hall*, Upper Saddle River, NJ, 1997.

[7] H. Ye, R.D. Degroat, "Maximum likelihood DOA estimation and asymptotic Cramer-Rao bounds for additive unknown colored noise," *IEEE Trans. on Signal Processing*, vol. 43, no. 4, pp. 938-949, April 1995.

[8] A.B. Gershman, P. Stoica, M. Pesavento, E.G. Larsson, "Stochastic Cramer-Rao bound for direction estimation in unknown noise fields," *IEE Proc.-Radar Sonar Navig.*, vol. 149, no. 1, pp. 2-8, February 2002.

[9] H. Abeida, J.P. Delmas, "Gaussian Cramer-Rao bound for direction estimation of noncircular signals in unknown noise fields," accepted to the *IEEE Transactions on Signal Processing*, 2005.

[10] H. Abeida, J.P. Delmas, "DOA MUSIC-like estimation for noncircular sources," submitted to the *IEEE Transactions on Signal Processing*, 2005.

[11] P. Stoica and A. Nehorai, "MUSIC, maximum likelihood, and Cramer-Rao bound: Further results and comparisons," *IEEE Transactions on ASSP*, vol. 38, no. 12, pp. 2140-2150, December 1990.

[12] P. Stoica and A. Eriksson, "MUSIC estimation of real-valued sine-wave frequencies," *Signal Processing*, vol. 42, pp. 139-146, 1995.

[13] P. Stoica, A. Eriksson and T. Söderström, "Optimally weighted MUSIC for frequency estimation," *SIAM J. Matrix Anal. Appl.*, vol. 16, no. 3, pp. 811-827, July 1995.

[14] J.P. Delmas, "Asymptotic performance of second-order algorithms," *IEEE Transactions on Signal Processing*, vol. 50, no. 1, pp. 49-57, January 2002.

[15] H. Abeida, J.P. Delmas, "Asymptotically minimum variance estimator in the singular case," accepted to *EUSIPCO, Antalya*, September 2005.

[16] J.P. Delmas, "Asymptotically minimum variance second-order estimation for noncircular signals with application to DOA estimation," *IEEE Trans. Signal Processing*, vol. 52, no. 5, pp. 1235-1241, May 2004.

[17] B. Ottersten, P. Stoica and R. Roy, "Covariance matching estimation techniques for array signal processing," *Digital Signal Processing*, vol. 8, pp. 185-210, July 1998.

[18] H. Abeida, J.P. Delmas, "Efficiency of subspace-based DOA estimation," submitted to the *IEEE Signal Processing Letters*, 2005.

[19] P. Stoica, A. Nehorai, "Performance study of conditional and unconditional direction of arrival estimation," *IEEE Trans. on Acoustics Speech and Signal Processing*, vol. 38, no. 10, pp. 1783-1795, Oct. 1990.

[20] B. Ottersten, M. Viberg and T. Kailath, "Analysis of subspace fitting and ML techniques for parameter estimation from sensor array data," *IEEE Trans. on Signal Processing*, vol. 40, no. 3, pp. 590-600, March 1992.

[21] A.J. Weiss, B. Friedlander, "On the Cramer-Rao bound for direction finding of correlated sources," *IEEE Trans. on Signal Processing*, vol. 41, no. 1, pp. 495-499, January 1993.

[22] P. Stoica, A.G. Larsson and A.B. Gershman, "The stochastic CRB for array processing: a textbook derivation," *IEEE Signal Processing letters*, vol. 8, no. 5, pp. 148-150, May 2001.

[23] M. Pesavento, A.B. Gershman, "Maximum-likelihood direction of arrival estimation in the presence of unknown nonuniform noise," *IEEE Trans. on Signal Processing*, vol. 49, no. 7, pp.1310-1324, July 2001.

[24] D. Slepian, "Estimation of signal parameters in the presence of noise," *in Trans. IRE Prof. Grop Inform. Theory PG IT-3*, pp. 68-89, 1954.

[25] W.J. Bangs "Array processing with generalized beamformers," *Ph.D. thesis Yale University, New Haven, CT*, 1971.

[26] J.P. Delmas, H. Abeida, "Stochastic Cramer-Rao bound for noncircular signals with application to DOA estimation," *IEEE Transactions on Signal Processing*, vol. 52, no. 11, pp. 3192-3199, November 2004.

[27] J.P. Delmas, H. Abeida, "Cramer-Rao bounds of DOA estimates for BPSK and QPSK modulated signals," accepted to the *IEEE Transactions on Signal Processing*, 2005.

[28] H. Abeida, J.P. Delmas, "Bornes de Cramer Rao de DOA pour signaux BPSK et QPSK en présence de bruit non uniforme," accepted to *GRETSI*, Louvain, 2005.

[29] S.T. Smith, "Statistical resolution limits and the complexified Cramer-Rao bound," *IEEE Trans. Signal Processing*, vol. 53, no. 5, pp. 1597-1609, May 2005.

[30] M. Kaveh, A.J. Barabell, "The statistical performance of MUSIC and the minimum-norm algorithms in resolving plane waves in noise," *IEEE Trans. Acoust. Speech, Signal Processing*, vol. 34, no. 2, pp. 331-341, April 1986.

[31] M. Lavielle, E. Moulines and J.F. Cardoso, "A maximum likelihood solution to DOA estimation for discrete sources," *Proc. Seventh IEEE Workshop on SP*, pp. 349-353, 1994.

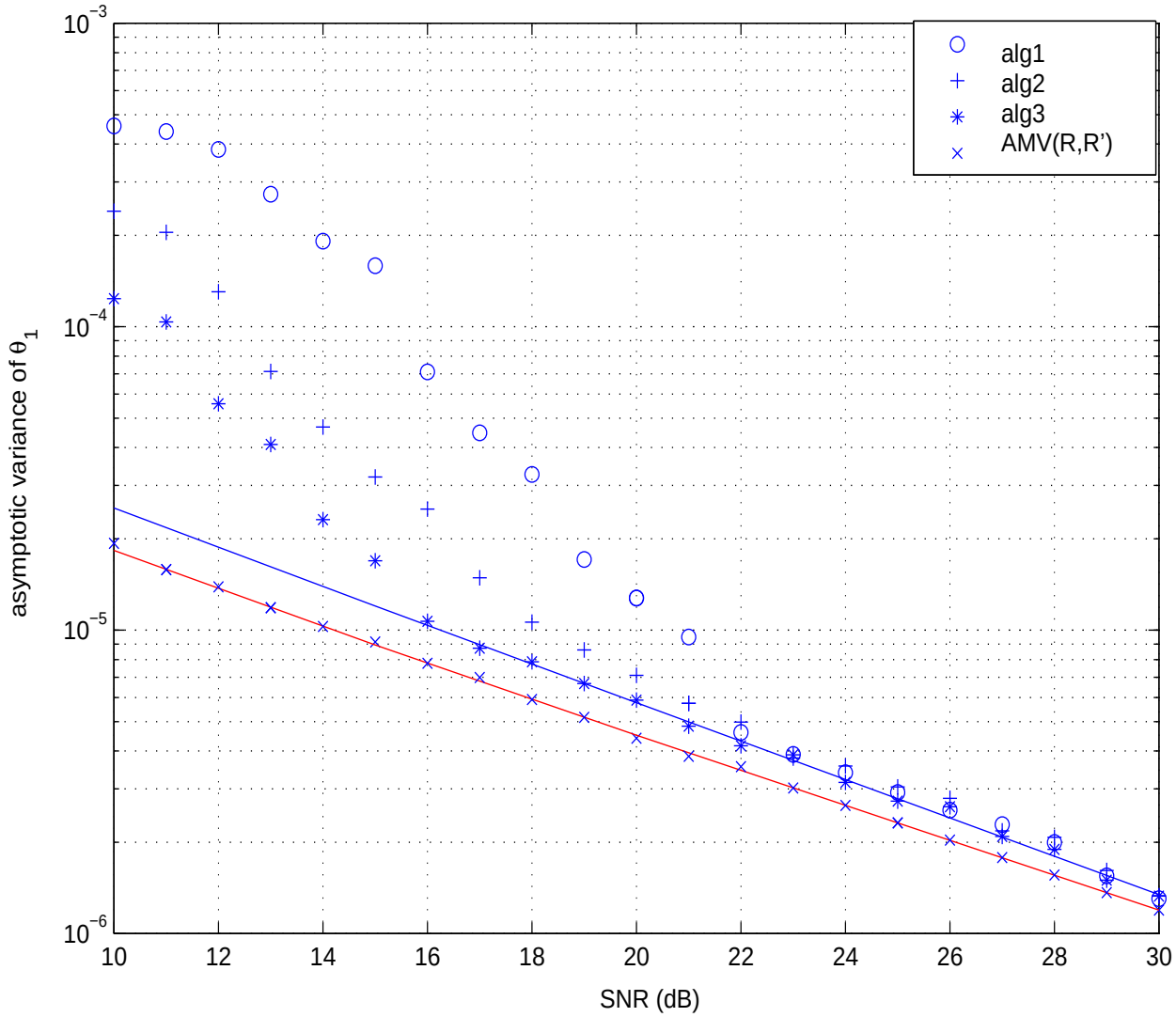

Fig.9.1 Theoretical (solid line) and empirical asymptotic variances given by algorithms 1, 2, 3 and AMV algorithms based on $(\mathbf{R}_{y,T}, \mathbf{R}'_{y,T})$ as a function of the SNR for $\Delta\theta = 0.05$rd, $\Delta\phi = \pi/6$rd.

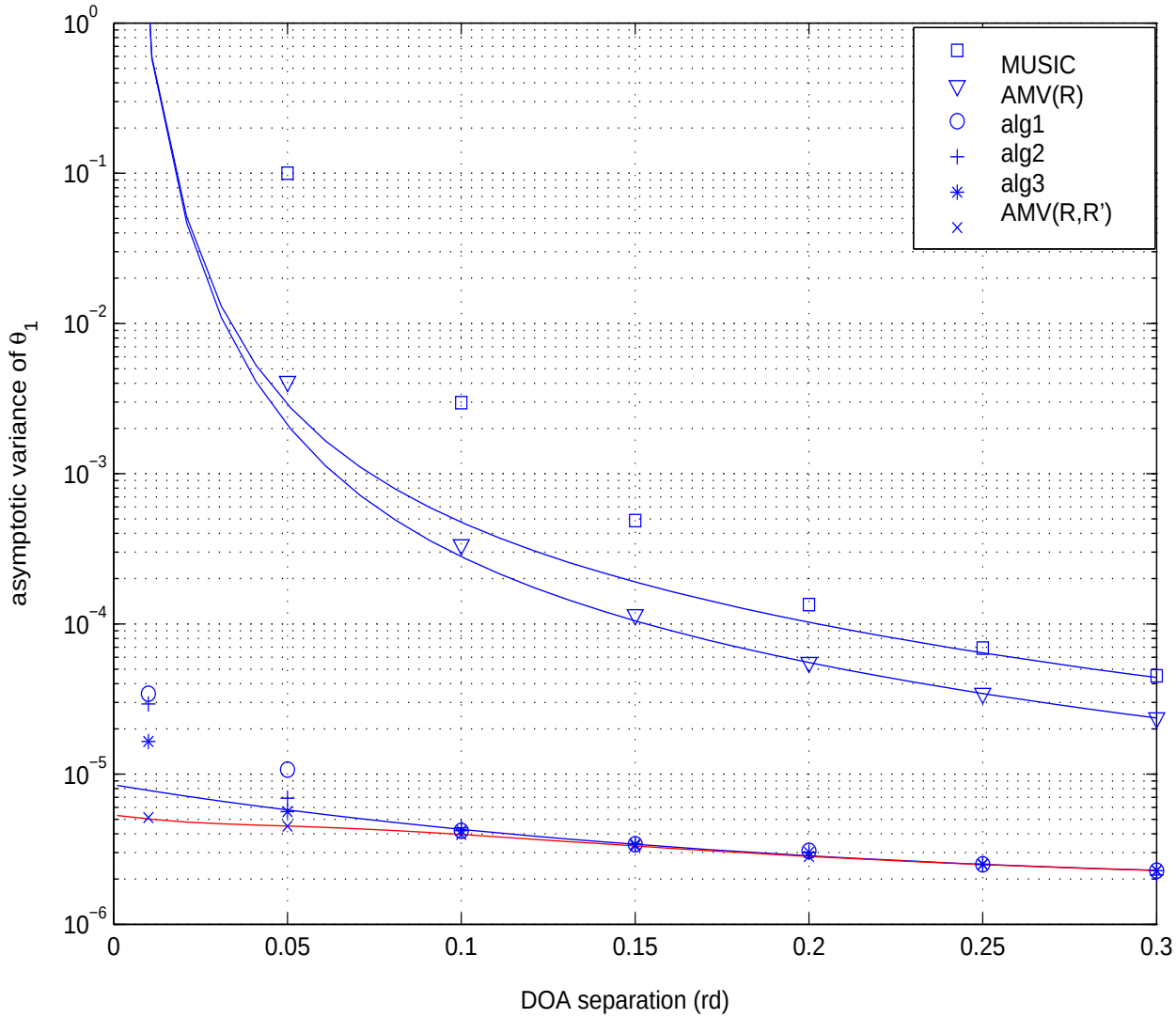

Fig.9.2 Theoretical (solid line) and empirical asymptotic variances given by algorithms 1, 2, 3, standard MUSIC and AMV algorithm based on $\mathbf{R}_{y,T}$ only and on $(\mathbf{R}_{y,T}, \mathbf{R}'_{y,T})$ as a function of the DOA separation for SNR=$20dB$, $\Delta\phi = \pi/6$rd.

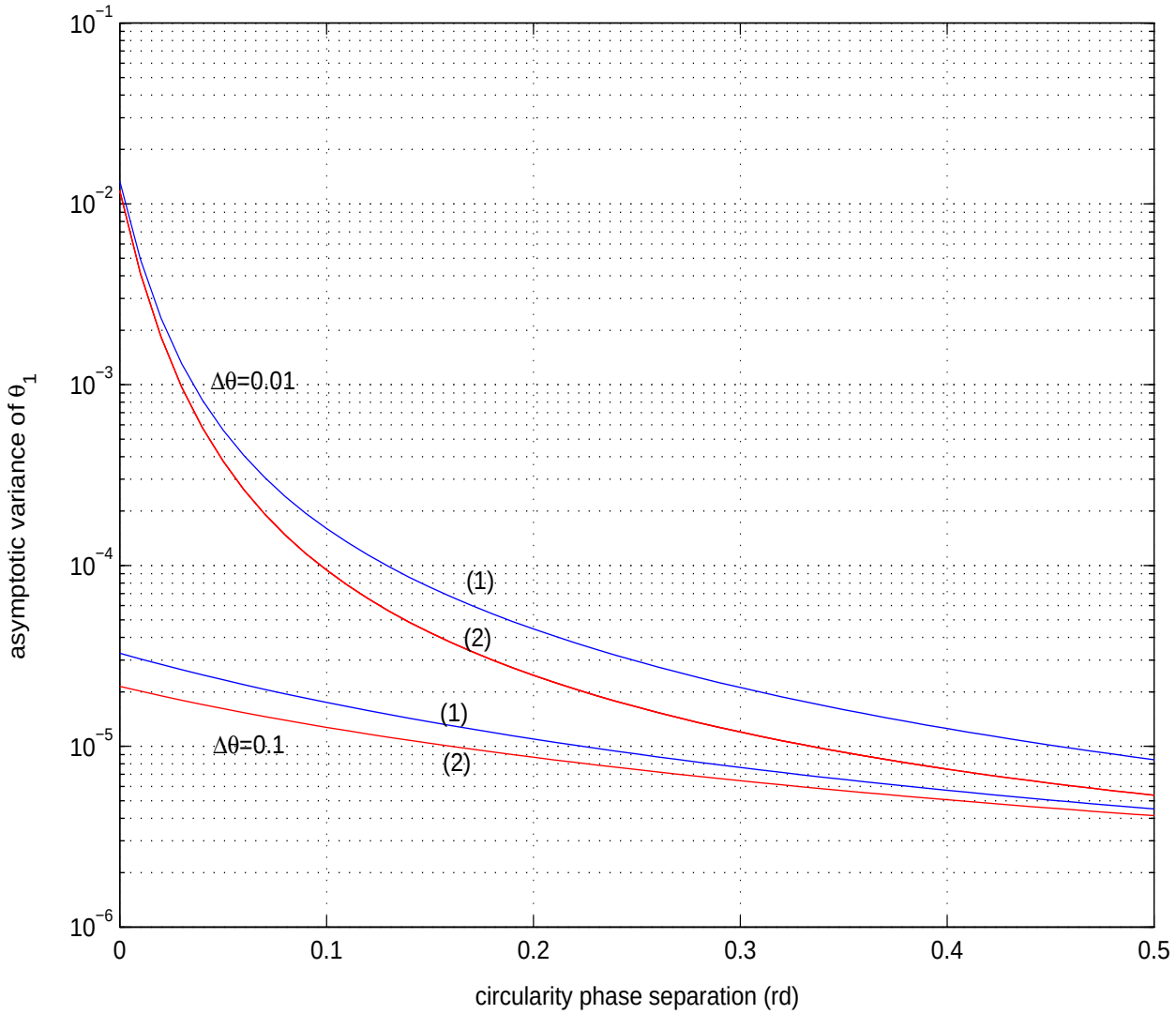

Fig.9.3 Theoretical asymptotic variances given by algorithms 1, 2, 3 (1) and by the AMV algorithm based on $(\mathbf{R}_{y,T}, \mathbf{R}'_{y,T})$ (2) as a function of the circularity phase separation for two DOA separations and SNR=$20dB$.

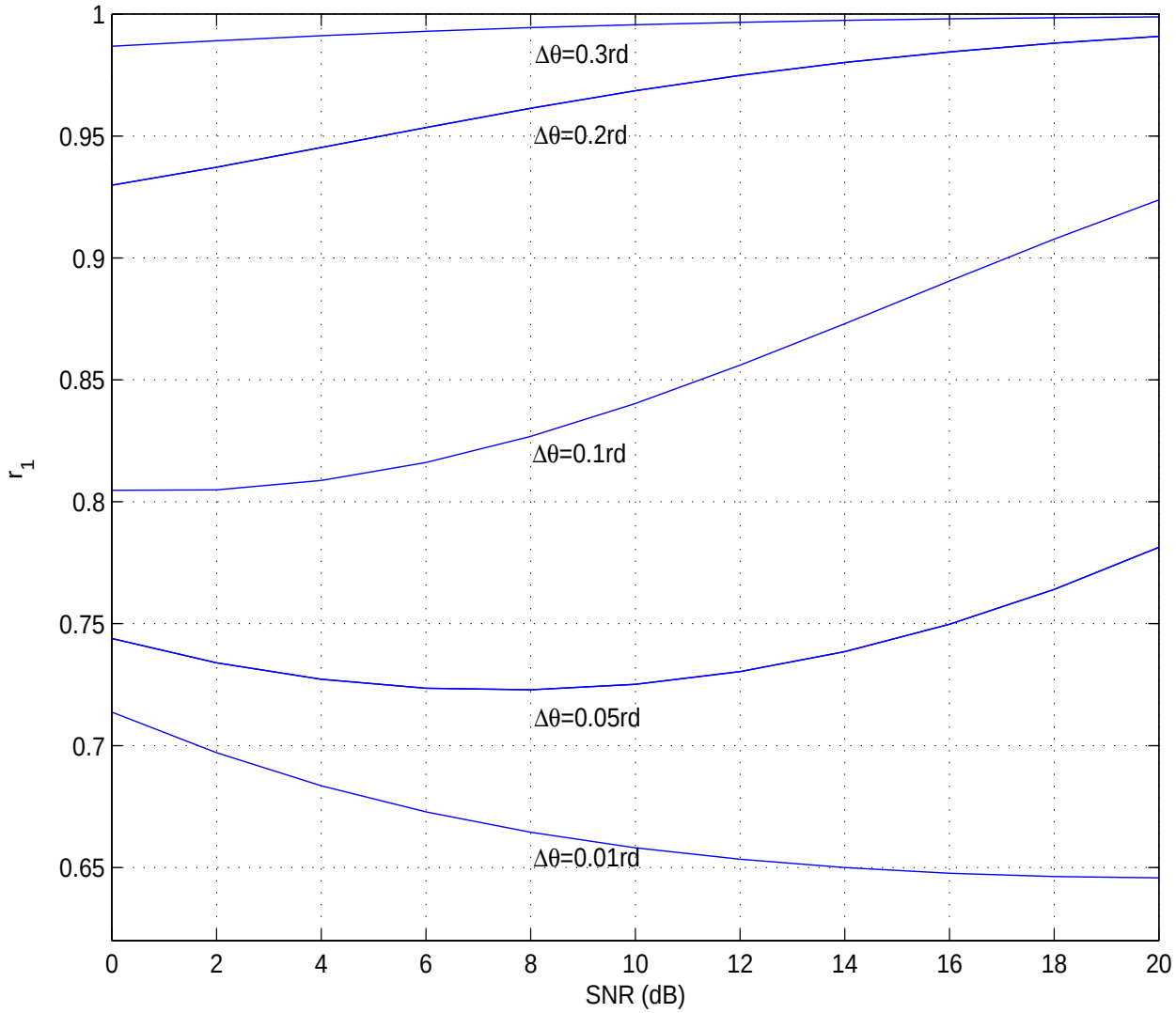

Fig.9.4 Ratio $r_1 \stackrel{\text{def}}{=} \text{Var}_{\theta_1}^{\text{AMV(R,R}')}/\text{Var}_{\theta_1}^{\text{Alg}_{1,2,3}}$ as a function of the SNR for different DOA separations, $\Delta\phi = \pi/6$rd.

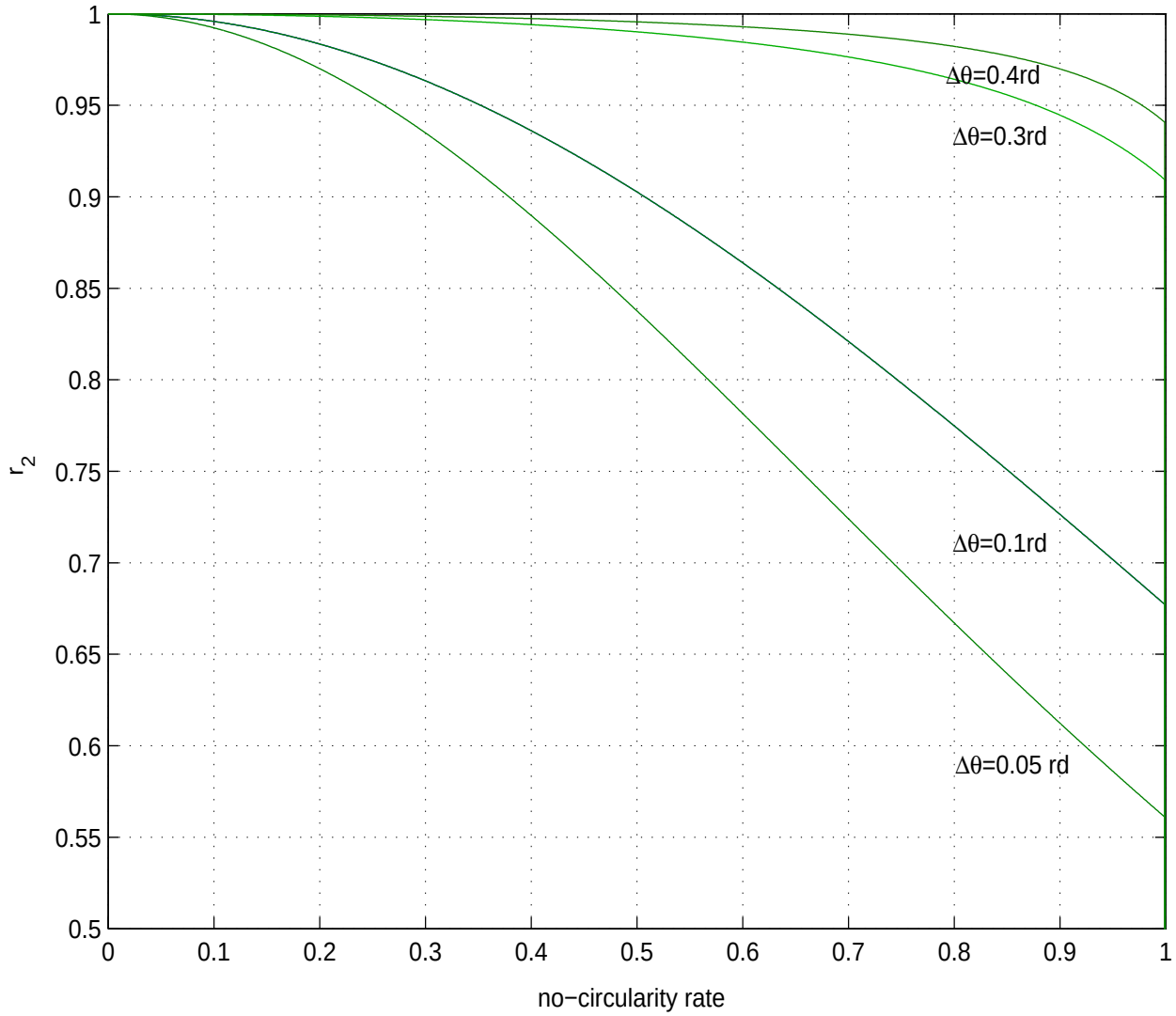

Fig.9.5 Ratio $r_2 \overset{\text{def}}{=} \text{Var}_{\theta_1}^{\text{Alg}_5}/\text{Var}_{\theta_1}^{\text{MUSIC(R)}}$ as a function of the noncircularity rate for different DOA separations for SNR=$5dB$.

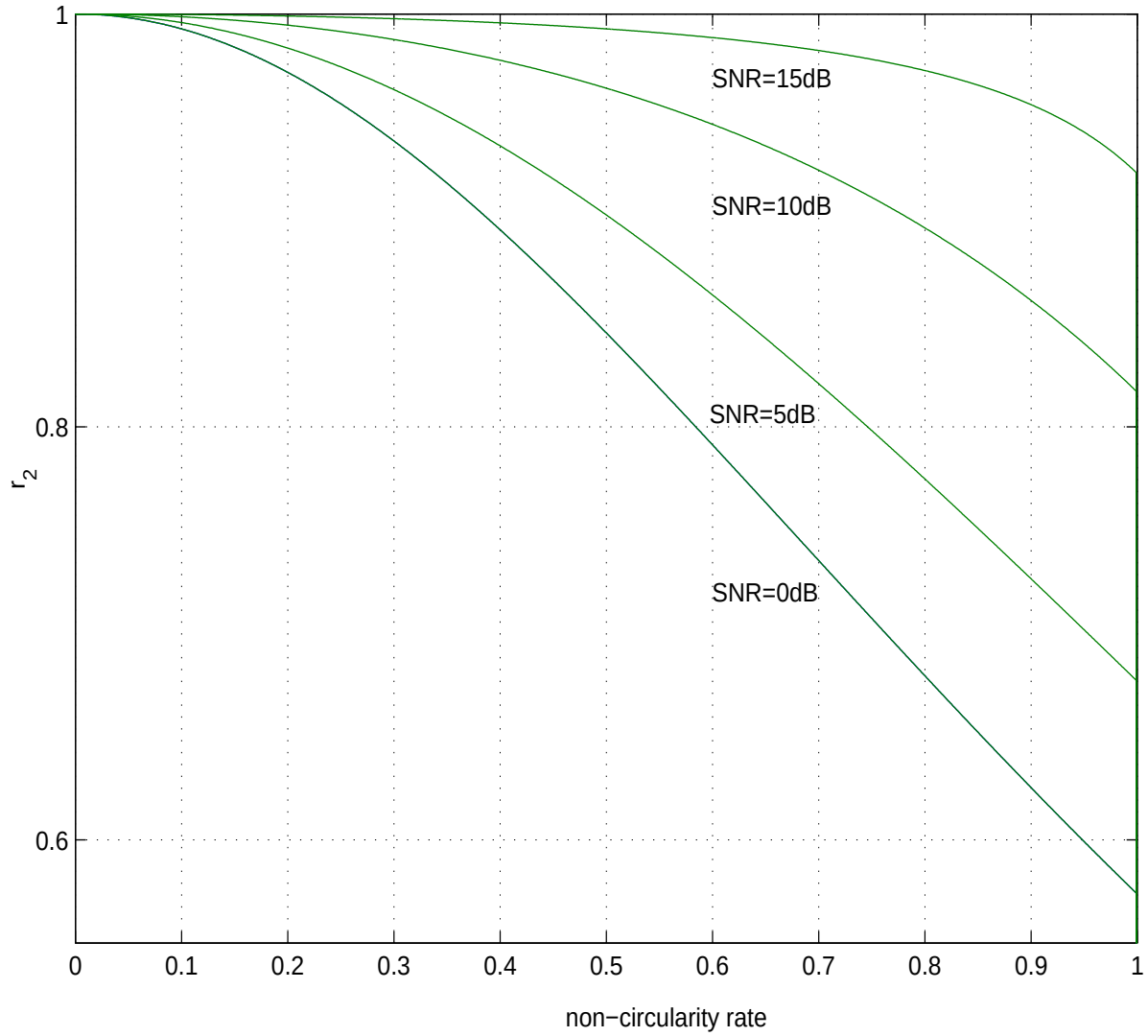

Fig.9.6 Ratio $r_2 \overset{\text{def}}{=} \text{Var}_{\theta_1}^{\text{Alg}_5}/\text{Var}_{\theta_1}^{\text{MUSIC(R)}}$ as a function of the noncircularity rate for different SNRs for $\Delta\theta = 0.1$rd.

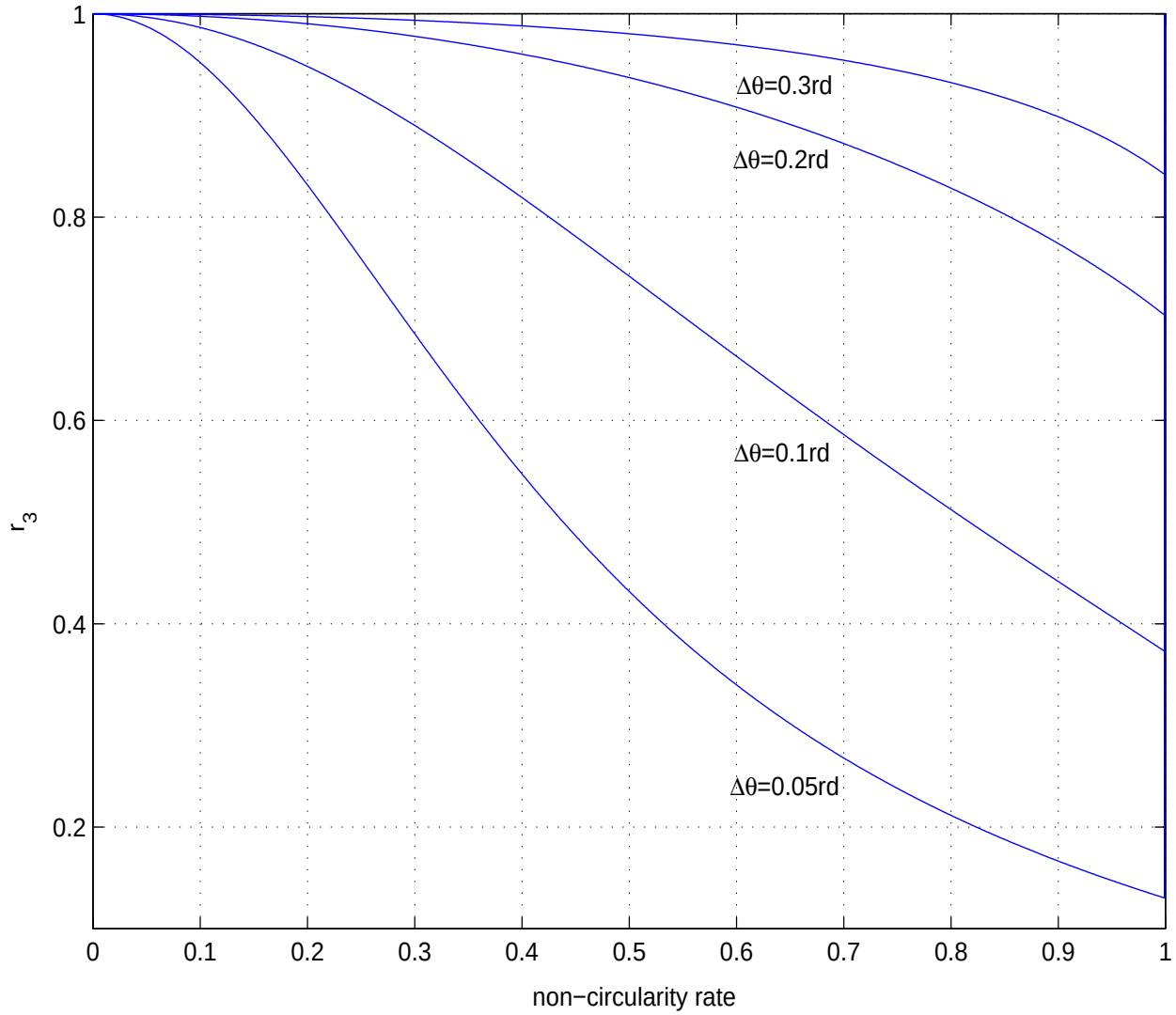

Fig.9.7 Ratio $r_3 \overset{\text{def}}{=} var_{\theta_1}^{\text{AMV(R,R}')}/var_{\theta_1}^{\text{AMV(R)}}$ as a function of the noncircularity rate for different DOA separations for SNR=$5dB$, $\alpha = \pi/2$rd and $\Delta\phi = \pi/6$rd.

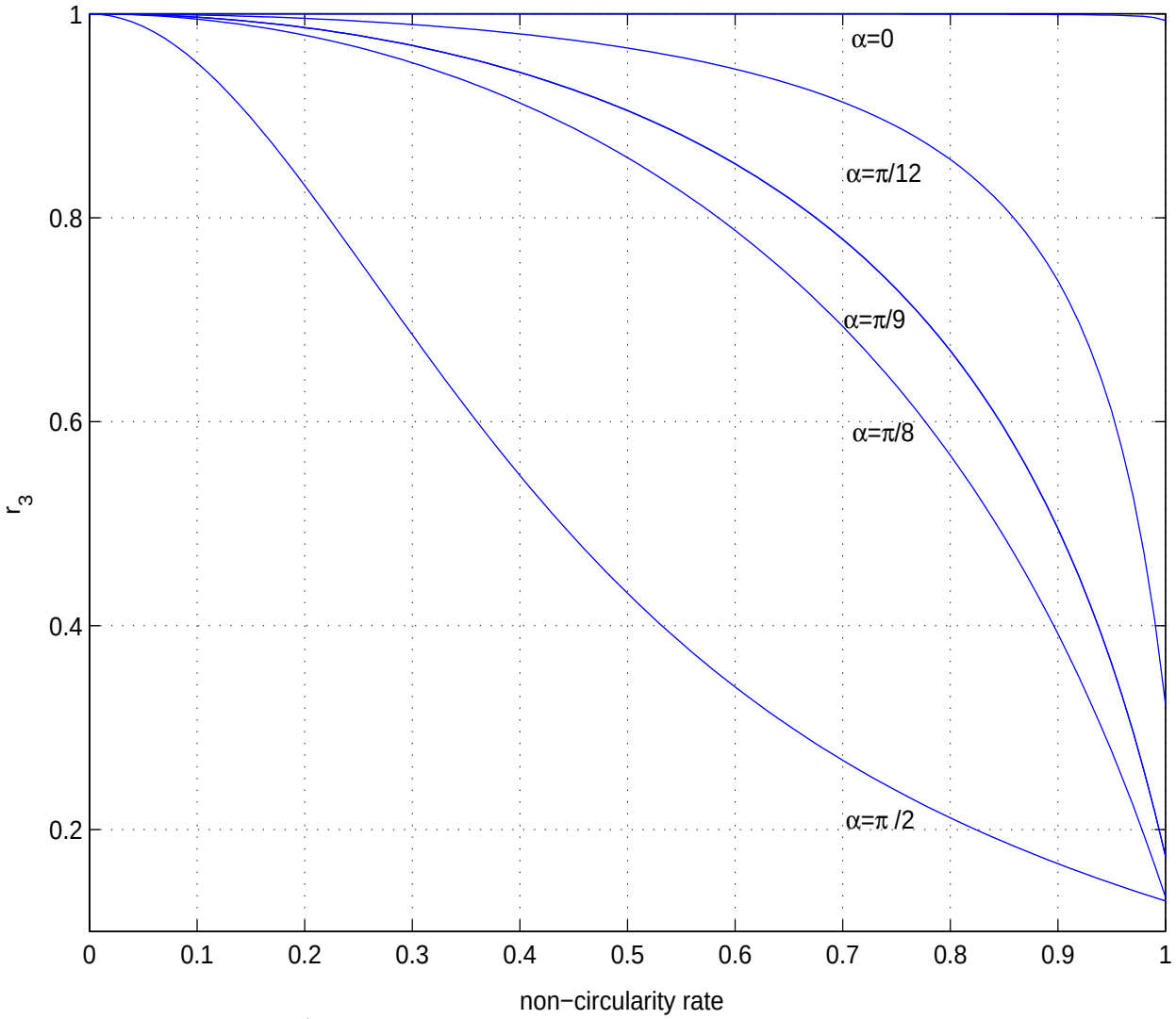

Fig.9.8 Ratio $r_3 \stackrel{\text{def}}{=} var_{\theta_1}^{\text{AMV(R,R}')}/var_{\theta_1}^{\text{AMV(R)}}$ as a function of the noncircularity rate for different spatial correlation α for SNR=$5dB$, $\Delta\theta = 0.1$rd and $\Delta\phi = \pi/6$rd.

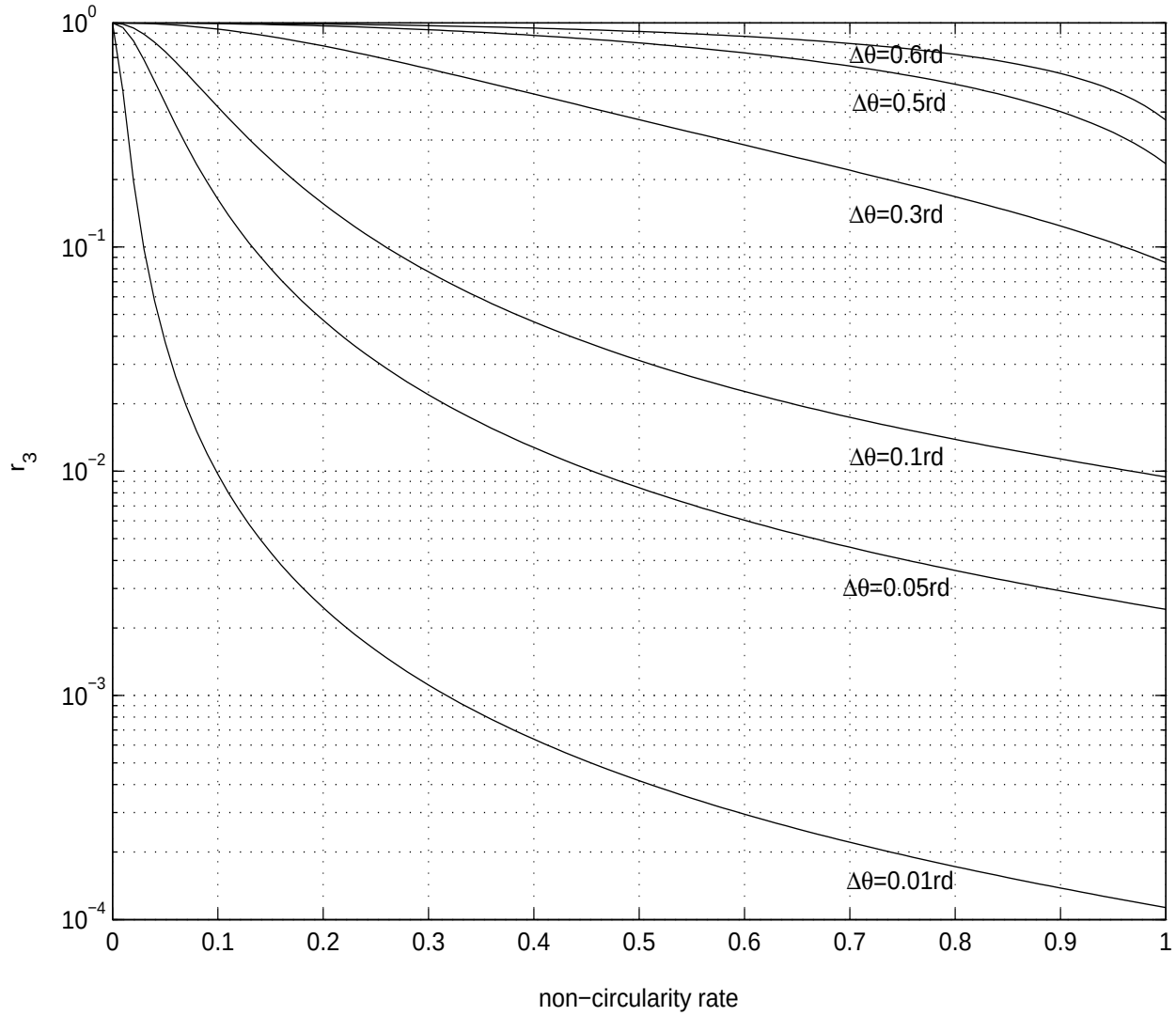

Fig.9.9 Ratio $r_3 \stackrel{\text{def}}{=} var_{\theta_1}^{\text{AMV(R,R}')}/var_{\theta_1}^{\text{AMV(R)}}$ as a function of the noncircularity rate for different DOA separations for SNR=5dB. $\Delta\phi = \pi/6$rd.

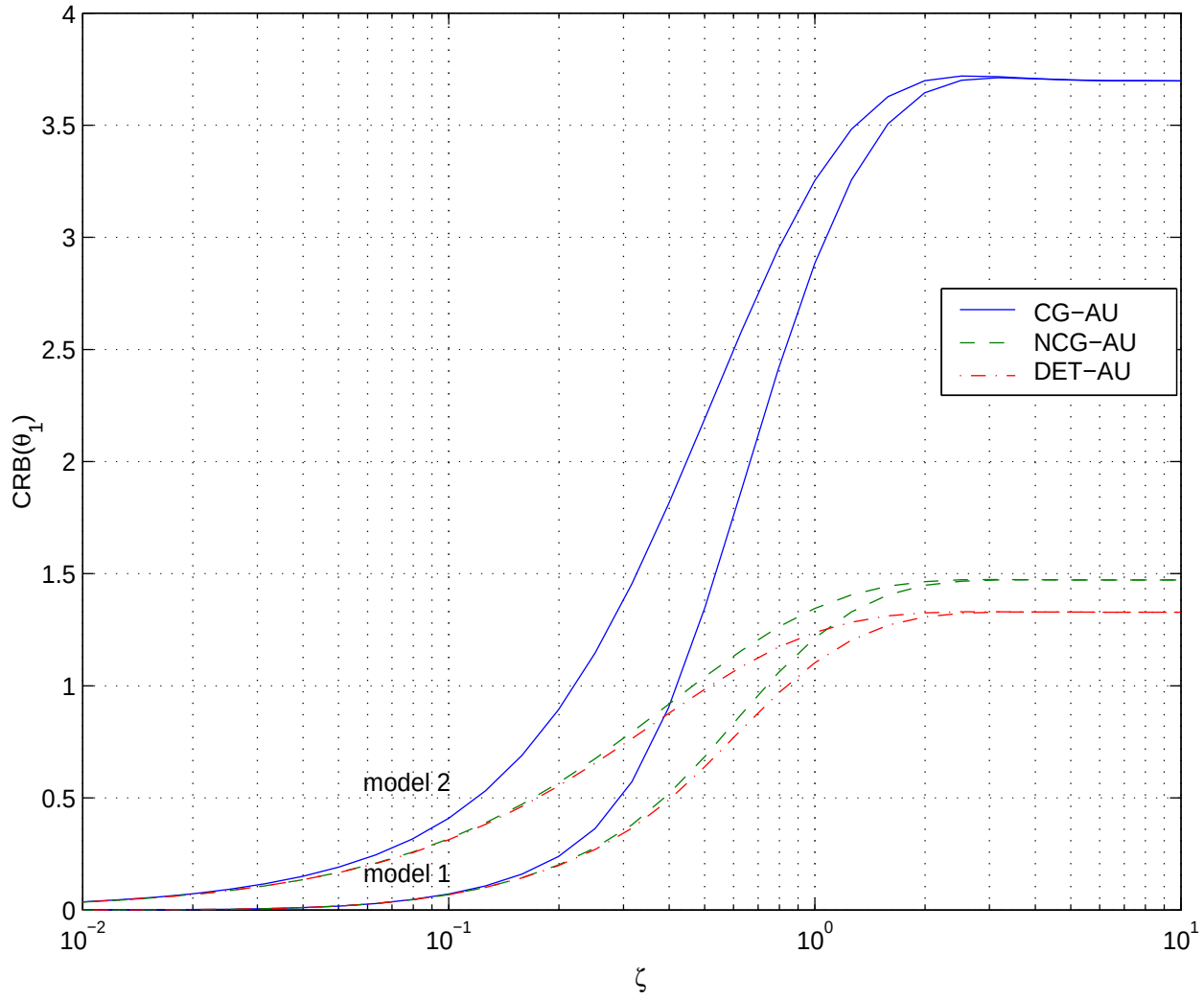

Fig.9.10 $\mathrm{CRB}_{\mathrm{AU}}^{\mathrm{NCG}}(\theta_1)$, $\mathrm{CRB}_{\mathrm{AU}}^{\mathrm{CG}}(\theta_1)$ and $\mathrm{CRB}_{\mathrm{AU}}^{\mathrm{DET}}(\theta_1)$ as a function of ζ for the first and second models with $\Delta\theta = 0.2rd$, SNR$= 0dB$ and $\Delta\phi = \pi/6$rd.

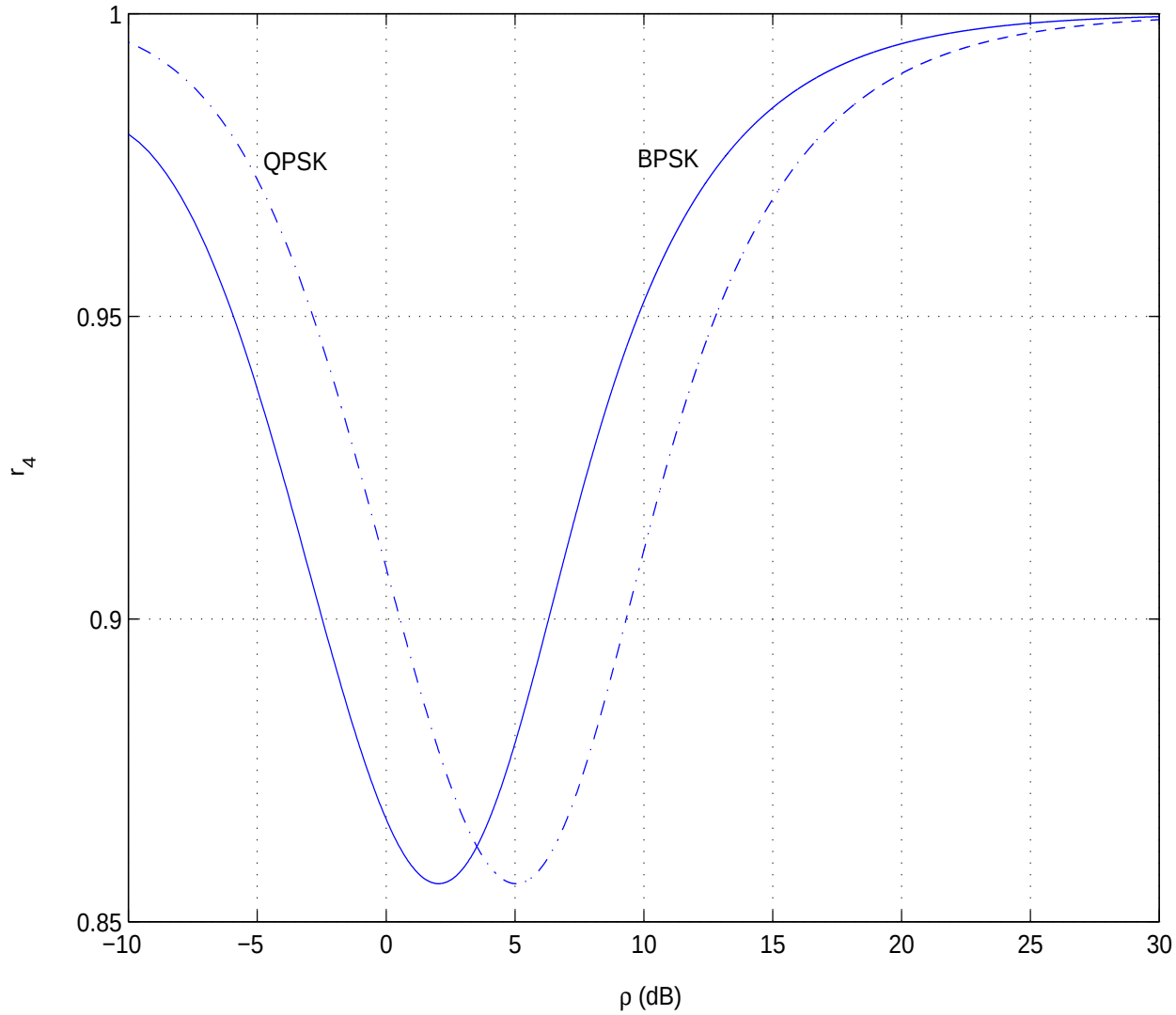

Fig.9.11 Ratios $r_4 \stackrel{\text{def}}{=} \frac{\text{CRB}_{\text{BPSK}}(\theta_1)}{\text{CRB}_{\text{NCG}}(\theta_1)}$ and $r_1(\theta_1) \stackrel{\text{def}}{=} \frac{\text{CRB}_{\text{QPSK}}(\theta_1)}{\text{CRB}_{\text{CG}}(\theta_1)}$ as a function of $\rho \stackrel{\text{def}}{=} Mr_1$.

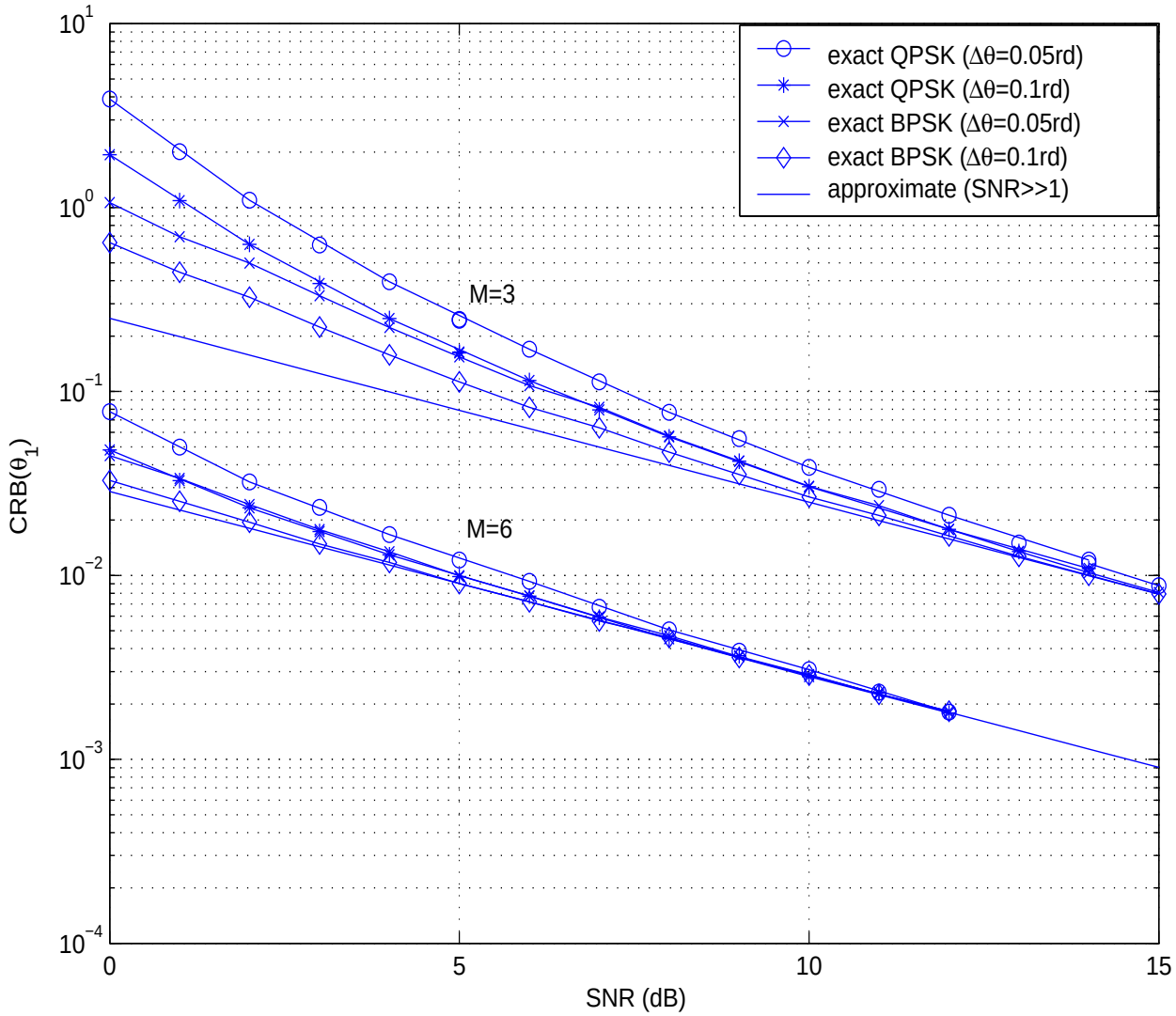

Fig.9.12 Approximate and exact value of $\mathrm{CRB}_{\mathrm{BPSK}}(\theta_1)$ and $\mathrm{CRB}_{\mathrm{QPSK}}(\theta_1)$ as a function of the SNR for different values of the DOA separation.

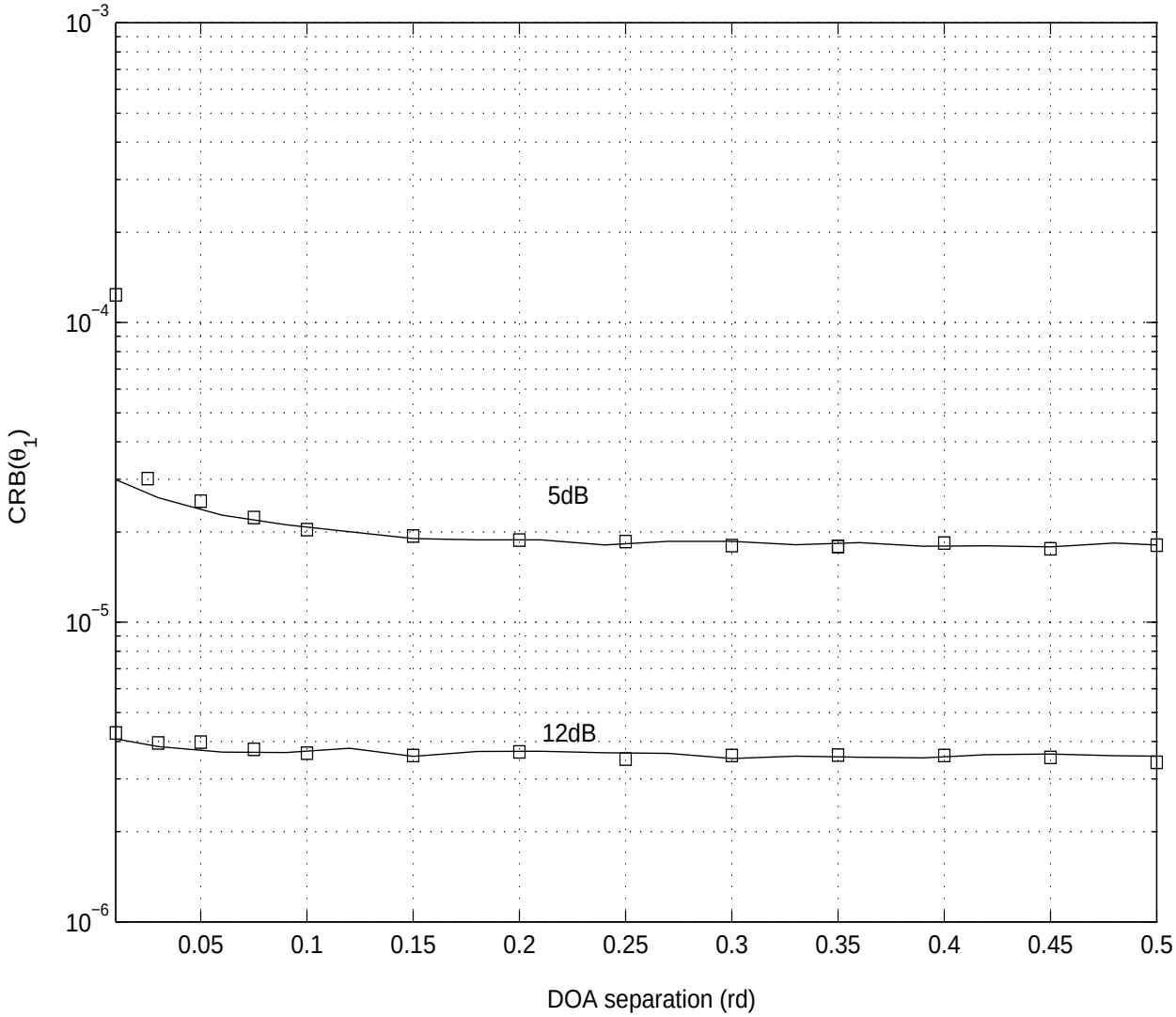

Fig.9.13 $\mathrm{CRB}_{\mathrm{BPSK}}(\theta_1)$ and estimated MSE $\mathrm{E}(\theta_{1,T} - \theta_1)^2$ given by the deterministic EM algorithm (10 iterations) as a function of the DOA separation for $\Delta\phi = 0.1$rd.

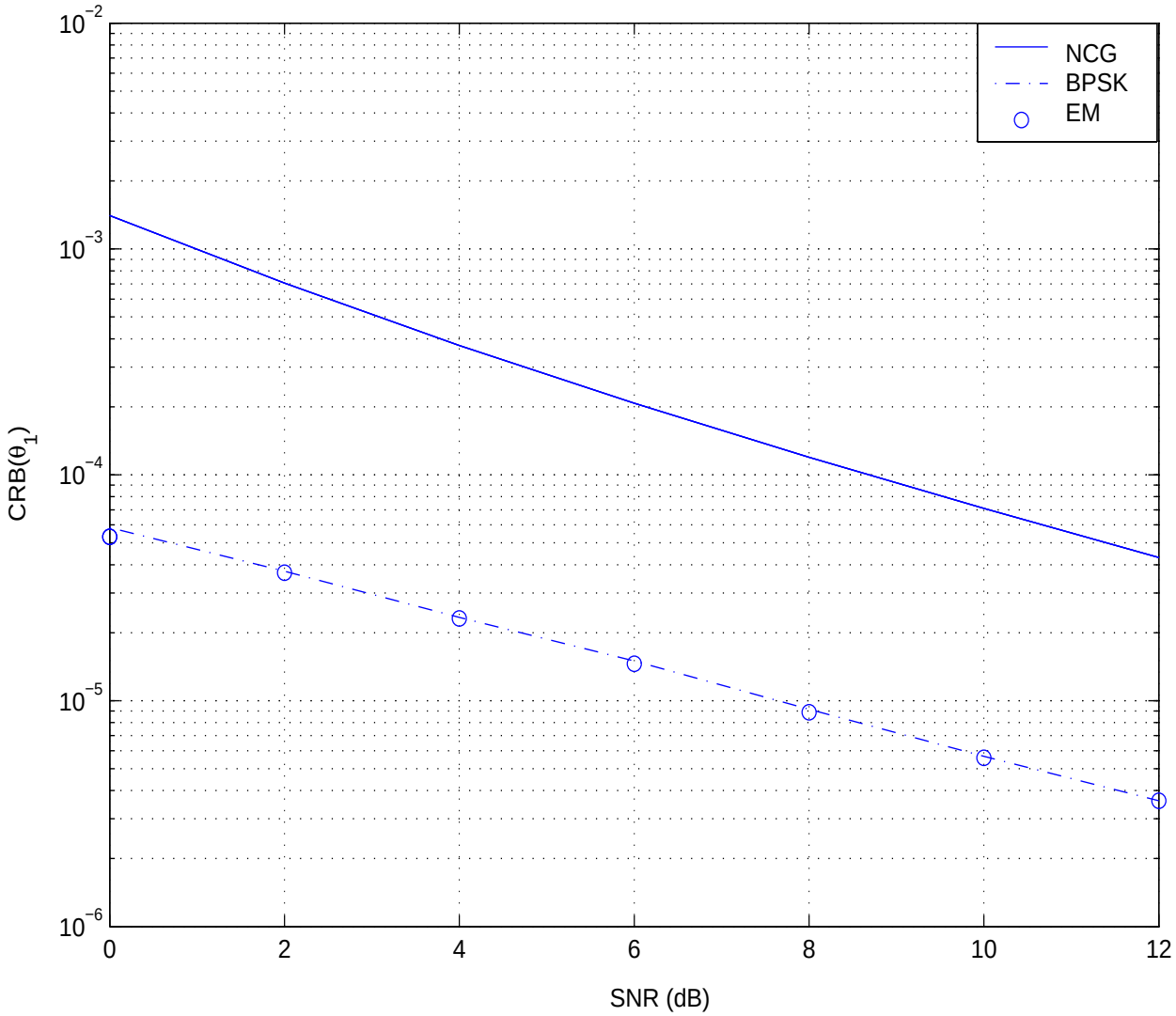

Fig.9.14 $\mathrm{CRB}_{\mathrm{BPSK}}(\theta_1)$, $\mathrm{CRB}_{\mathrm{NCG}}(\theta_1)$ and estimated MSE $\mathrm{E}(\theta_{1,T} - \theta_1)^2$ given by the deterministic EM algorithm (5 iterations), for $\Delta\theta = 0.3rd$ and $\Delta\phi = 0.1$rd, versus SNR.

Biographies of the authors

Jean Pierre Delmas was born in France in 1950. He received the Engineering degree from Ecole Centrale de Lyon, France in 1973, the Certificat d'études supérieures from the Ecole Nationale Supérieure des Télécommunications, Paris, France in 1982 and the Habilitation à diriger des recherches (HDR) degree from the University of Paris, Orsay, France in 2001. Since 1980, he has been with the Institut National des Télécommunications where he is presently a Professor in the CITI department and in UMR-CNRS 5157. His teaching and research interests are in the areas of statistical signal processing with application to communications and antenna array. He is currently an Associate Editor for the IEEE Transactions on Signal Processing.

Habti Abeida was born in Settat, Morocco in 1977. He received the Mastery engineering degrees in applied mathematics from Hassan II university, Casablanca, Morocco in 2000 and from René Descartes University, Paris, France in 2001 respectively, and Master's degree in Statistics from Pierre et Marie Curie university, Paris, France, in 2002. He is currently pursuing the Ph.D. degree in applied mathematics and digital communications in the Institut National des Télécommunications, Evry, France. His research interests are in statistical signal processing.